

Characterization of the role of single domain soybean cystatins in regulating drought responses in soybean

By

Zaheer Karriem



A thesis submitted in partial fulfilment of the requirements for the degree of Magister Scientiae (Biotechnology) in the Department of Biotechnology, University of the Western Cape.

Supervisor: Prof. Ndiko Ludidi

December 2015

Characterization of the role of single domain soybean cystatins in regulating drought responses in soybean

Zaheer Karriem

Keywords

Caspase-like activity

Cystatins

Cysteine proteases

Drought

Gene expression

Glycine max

Programmed cell death

Protein overexpression

Reactive oxygen species



ABSTRACT

This study investigated the effects that drought stress imposed on the growth and development of soybean plants. Soybeans were initially observed at the whole-plant level in order to identify the physical changes that had taken place in response to drought. Further investigation of the effects of drought stress on Soybean plants were quantified at the molecular level.

Physical changes of soybeans in response to drought stress were typified by the change in leaf morphology and pigmentation. At the molecular level, it was observed that drought stress resulted in the accumulation of hydrogen peroxide in soybean leaves, which was met by elevated levels of lipid peroxidation.

The effects of drought on the modulation of (and interplay between cystatins) cysteine protease (caspase-like) activity and programmed cell death (PCD) were also investigated. Total caspase-like activity and cell death were enhanced in response to water deficit despite the up-regulation in gene expression of the cystatin Glyma14g04250. The cystatin Glyma18g12240 was not expressed in soybean leaves, whilst the gene expression of the cystatin Glyma20g08800 remained unchanged in response to drought.

This study was aimed at the characterization of two single domain soybean cystatins, namely, Glyma14g04250 and Glyma20g08800 which could potentially be overexpressed in transgenic soybean plants in an attempt to alleviate the effects of drought stress.

DECLARATION

I declare that “Characterization of the role of single domain soybean cystatins in regulating drought responses in soybean” is my own work, that it has not been submitted for any degree or examination in any other university, and that all the sources I have used or quoted have been indicated and acknowledged by complete references.

Full name..... Date.....

Signed.....

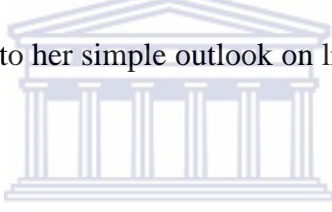


ACKNOWLEDGEMENTS

I would like to thank all the individuals that have helped me in achieving everything that I have accomplished thus far.

First and foremost, I would like to give thanks to my mother **Jasmine Karriem** for all of her efforts and endeavours in supporting me throughout my life. My brothers, **Hishaam Manuel**, **Khaleel Manuel**, **Shameer Karriem** and **Yasseen Karriem** for bringing me much needed joy and support.

A constant source of inspiration and motivation to continue my studies were ever-present from my niece **Sarah Karriem** (Age 5) due to her simple outlook on life, making any potential difficulties seem irrelevant and laughable.



My close friends **Edgar Moralie** and **Fathima Osman** are individuals that have helped me mold my character into the hardworking and goal driven person that I have become.

Professor **Ndiko Ludidi** has become a role-model for me during the short time that I know him. He has in many ways made me the scientist that I am today, and I aspire to continue reaching new heights by fulfilling my potential through his guidance.

The individuals I have mentioned, and various others, have been the driving force to my insatiable desire for obtaining knowledge and wisdom through my education.

In closing, I am particularly thankful to the **National Research Foundation (NRF)**, for funding my studies and allowing me to achieve my aspirations in the field of science, as well as the **University of the Western Cape** for providing me with this platform.

TABLE OF CONTENTS

ABSTRACT.....	II
DECLARATION	III
ACKNOWLEDGEMENTS	IV
TABLE OF CONTENTS	V
LIST OF ABBREVIATIONS	IX
LIST OF FIGURES	X
LIST OF TABLES.....	XI
AIMS AND OBJECTIVES OF THE STUDY	XI
CHAPTER 1: LITERATURE REVIEW	1
1.1 INTRODUCTION	1
1.2 REACTIVE OXYGEN SPECIES	3
1.3 PRODUCTION OF ROS IN PLANTS.....	3
1.3.1 CHLOROPLASTS AND ROS GENERATION.....	4
1.3.2 MITOCHONDRIA AND ROS GENERATION	5
1.3.3 PEROXISOMES AND ROS GENERATION.....	7
1.4 SIGNIFICANCE AND ROLES OF ROS IN PLANT SIGNALING AND OXIDATIVE STRESS.....	9
1.4.1 SUPEROXIDE AS A SIGNALING MOLECULE	10
1.4.2 HYDROGEN PEROXIDE AS A SIGNALING MOLECULE	10
1.5 ROS INDUCED OXIDATIVE STRESS.....	11
1.5.1 LIPID PEROXIDATION (LPO).....	11
1.5.2 OXIDATION OF PROTEINS	12
1.5.3 DNA DAMAGE	13
1.6 ANTIOXIDANT DEFENCE MECHANISMS	14
1.6.1 NON-ANTIOXIDANT DETOXIFICATION PATHWAYS.	15
1.6.2 ENZYMATIC DETOXIFICATION PATHWAYS.....	16
1.6.2.1 SUPEROXIDE DISMUTASE (SOD)	16
1.6.2.2 ASCORBATE PEROXIDASE (APX)	17
1.7 REGULATION OF ANTIOXIDANTS AND ROS.....	18
1.8 PROGRAMMED CELL DEATH AND NECROSIS IN PLANTS.....	20
1.8.1 NECROSIS IN PLANTS	21
1.8.2 PROGRAMMED CELL DEATH IN PLANTS	21
1.9 CYSTEINE PROTEASES AND THEIR ROLES IN THE PCD PATHWAYS	22
1.10 CYSTATINS AND THEIR BIOLOGICAL IMPORTANCE IN PLANTS	23
1.11 MODE OF ACTION OF CYSTATINS	23
1.12 CYSTEINE PROTEASES, CYSTATINS AND PCD INTERPLAY.....	24
CHAPTER 2: DROUGHT-INDUCED CHANGES IN <i>GLYCINE MAX</i> PHYSIOLOGYAND	

BIOCHEMISTRY AT THE V3 AND R1 DEVELOPMENTAL STAGES.....	26
ABSTRACT.....	26
2.1 INTRODUCTION	27
2.2 MATERIALS AND METHODS.....	28
2.2.1 GERMINATION AND GROWTH OF <i>GLYCINE MAX</i>	28
2.2.2 GROWTH OF <i>GLYCINE MAX</i> UNTIL THE V3 DEVELOPMENTAL STAGE	28
2.2.3 GROWTH OF <i>GLYCINE MAX</i> UNTIL THE R1 DEVELOPMENTAL STAGE	29
2.2.4 MEASUREMENT OF CHANGES IN SOYBEAN PHYSICAL PARAMETERS	29
2.2.5 MEASUREMENT OF DROUGHT-INDUCED MOLECULAR LEVEL CHANGES IN SOYBEAN AT THE V3 DEVELOPMENTAL STAGE	29
2.2.5.1 RELATIVE WATER CONTENT ASSAY	30
2.2.5.2 METABOLITE EXTRACTION (TCA EXTRACTION).....	30
2.2.5.3 HYDROGEN PEROXIDE CONTENT IN SOYBEAN LEAVES.....	30
2.2.5.4 LIPID PEROXIDATION IN SOYBEAN LEAVES	31
2.2.5.5 TOTAL CASPASE-LIKE ACTIVITY IN SOYBEAN LEAVES.....	31
2.2.5.6 CELL VIABILITY ASSAY FOR SOYBEAN LEAVES.....	32
2.2.5.7 ANALYSIS OF GLYMA14G04250, GLYMA18G12240 AND GLYMA20G08800 GENE EXPRESSION	33
2.2.5.7.1 EXTRACTION OF TOTAL RNA FROM SOYBEAN LEAVES	33
2.2.5.7.2 DNASE TREATMENT OF TOTAL RNA SAMPLES	34
2.2.5.7.3 FIRST STRAND cDNA SYNTHESIS FROM DNASE-TREATED RNA SAMPLES.....	34
2.2.5.7.4 SEMI-QUANTITATIVE PCR ANALYSIS OF GENE EXPRESSION FOR GLYMA14G04250, GLYMA18G12240 AND GLYMA20G08800 RELATIVE TO 18S RNA	35
2.2.5.7.5 QUANTITATIVE REAL-TIME PCR ANALYSIS OF GLYMA14G04250, GLYMA18G12240 AND GLYMA20G08800 GENE EXPRESSION.....	36
2.3 RESULTS	37
2.3.1 DROUGHT-INDUCED CHANGES IN SOYBEAN LEAF MORPHOLOGY	37
2.3.2 MEASUREMENT OF CHANGES IN SOYBEAN PHYSICAL PARAMETERS	38
2.3.2.1 CHANGES IN SHOOT LENGTHS FOR SOYBEAN PLANTS IN RESPONSE TO DROUGHT STRESS	39
2.3.2.2 CHANGES IN NUMBER OF STEM NODES FOR SOYBEAN PLANTS IN RESPONSE TO DROUGHT STRESS.....	40
2.3.3 MEASUREMENT OF DROUGHT-INDUCED MOLECULAR LEVEL CHANGES IN SOYBEAN	41
2.3.3.1 QUANTIFICATION OF DROUGHT-INDUCED CHANGES IN THE RELATIVE WATER CONTENT OF SOYBEAN LEAVES.....	41
2.3.3.2 MEASUREMENT OF DROUGHT-INDUCED CHANGES IN HYDROGEN PEROXIDE CONTENT IN SOYBEAN LEAVES.....	42
2.3.3.3 MEASUREMENT OF DROUGHT-INDUCED CHANGES IN LIPID PEROXIDATION VIA DETECTION OF MALONDIALDEHYDE CONTENT IN SOYBEAN LEAVES.....	44
2.3.3.4 QUANTIFICATION OF TOTAL CASPASE-LIKE ACTIVITY IN SOYBEAN LEAVES IN RESPONSE TO WATER DEFICIT	45

2.3.3.5 MEASUREMENT OF CHANGES IN CELL DEATH OF SOYBEAN LEAVES IN RESPONSE TO WATER DEFICIT	46
2.3.3.6 ANALYSIS OF DROUGHT-INDUCED CHANGES IN RELATIVE GENE EXPRESSION OF GLYMA14G04250, GLYMA18G12240 AND GLYMA20G08800 VIA SEMI-QUANTITATIVE RT-PCR	47
2.3.3.7 REAL-TIME ANALYSIS OF DROUGHT-INDUCED CHANGES IN RELATIVE GENE EXPRESSION FOR GLYMA14G04250 AND GLYMA20G08800 VIA qPCR.....	50
2.4 DISCUSSION	51
2.5 CONCLUSIONS.....	53

CHAPTER 3: CHARACTERIZATION OF TWO SINGLE DOMAIN CYSTATINS, GLYMA14G04250 AND GLYMA20G08800 FROM <i>GLYCINE MAX</i>	55
ABSTRACT.....	55
3.1 INTRODUCTION	56
3.2 MATERIALS AND METHODS	57
3.2.1 PCR AMPLIFICATION AND SEQUENCING OF GLYMA14G04250 AND GLYMA20G08800	57
3.2.1.1 IDENTIFICATION AND PROBE DESIGN OF GLYMA14G04250 AND GLYMA20G08800 USING BLAST	57
3.2.1.2 EXTRACTION OF TOTAL RNA FROM SOYBEAN LEAVES	57
3.2.1.3 DNASE TREATMENT OF TOTAL RNA SAMPLES.....	58
3.2.1.4 FIRST STRAND cDNA SYNTHESIS	59
3.2.1.5 OPTIMIZATION OF ANNEALING TEMPERATURES FOR PRIMER-SPECIFIC PCR AMPLIFICATION OF GLYMA14G04250 AND GLYMA20G08800	59
3.2.1.6 HIGH-FIDELITY PCR AMPLIFICATION OF FULL-LENGTH SOYBEAN CYSTATIN GENES	60
3.2.1.7 AGAROSE GEL ELECTROPHORESIS, GEL PURIFICATION AND SEQUENCING OF CYSTATIN GENES	61
3.2.2 BACTERIAL OVEREXPRESSION OF GLYMA14G04250 AND GLYMA20G08800.....	61
3.2.2.1 CLONING OF GLYMA14G04250 AND GLYMA20G08800 INTO pET44a VECTOR	61
3.2.2.2 TRANSFORMATION AND GROWTH OF <i>E.COLI</i> DH5 α	62
3.2.2.3 COLONY PCR AMPLIFICATION OF GLYMA14G04250 AND GLYMA20G08800 FROM <i>E.COLI</i> DH5 α	63
3.2.2.4 SELECTIVE GROWTH OF TRANSFORMED <i>E.COLI</i> DH5 α	63
3.2.2.5 ISOLATION OF PLASMID CONSTRUCTS FROM <i>E.COLI</i> DH5 α	64
3.2.2.6 TRANSFORMATION AND GROWTH OF <i>E.COLI</i> BL21	64
3.2.2.7 COLONY PCR AMPLIFICATION OF GLYMA14G04250 AND GLYMA20G08800 FROM <i>E.COLI</i> BL21	65
3.2.2.8 SELECTIVE GROWTH OF TRANSFORMED <i>E.COLI</i> BL21 AND OVEREXPRESSION OF GLYMA14G04250 AND GLYMA20G08800	66
3.2.3 ISOLATION AND PURIFICATION OF GLYMA14G04250 AND GLYMA20G08800	67
3.2.3.1 ISOLATION OF TOTAL PROTEIN FROM <i>E.COLI</i> BL21	67
3.2.3.2 AFFINITY CHROMATOGRAPHY PURIFICATION OF GLYMA14G04250 AND GLYMA20G08800 RECOMBINANT PROTEINS.....	67

3.2.3.3 CLEAVAGE OF RECOMBINANT PROTEINS AND PURIFICATION OF GLYMA14G04250 AND GLYMA20G08800	68
3.2.3.4 ANALYSIS OF PURIFIED PROTEINS VIA SDS-PAGE GEL ELECTROPHORESIS	69
3.2.3.5 CHARACTERIZATION OF GLYMA14G04250 AND GLYMA20G08800 ACTIVITY	69
3.3 RESULTS	70
3.3.1 SCREENING OF TRANSFORMED <i>E.COLI</i> DH5 α AND BL21 FOR TARGET GENES	70
3.3.2 SDS-PAGE ANALYSIS OF PROTEIN PURIFICATION BY AFFINITY CHROMATOGRAPHY.	72
3.3.3 DETECTION OF GLYMA14G04250 AND GLYMA20G08800 INHIBITORY ACTION ON TOTAL CASPASE-LIKE ACTIVITY FROM SOYBEAN LEAVES	73
3.4 DISCUSSION	75
3.5 CONCLUSIONS.....	76
BIBLIOGRAPHY	77



LIST OF ABBREVIATIONS

ANOVA	Analysis of variance
APX	Ascorbate peroxidase
AsA	Ascorbic acid
BLAST	Basic Local Alignment Search Tool
DNA	Deoxyribonucleic acid
dNTPs	Dinucleosidetriphosphates
DTT	Dithiothreitol
<i>E.coli</i>	<i>Escherischia coli</i>
EDTA	Ethylenediaminetetraacetic acid
EtOH	Ethanol
FW	Fresh weight
IPTG	Isopropyl β-D-thiogalactosidase
LB	Luria-Bertani
LPO	Lipid peroxidation
MDA	Malondialdehyde
NBT	Nitro tetrazolium blue
OD	Optical density
PAGE	Polyacrylamide gel electrophoresis
PVPP	Polyvinylpolypyrrolidone
PUFA	Polyunsaturated fatty acid
RT-PCR	Reverse transcription Polymerase chain reaction
qPCR	Quantitative real time Polymerase Chain Reaction
RNA	Ribonucleic acid
ROS	Reactive oxygen species
RWC	Relative water content
SOD	Superoxide dismutase
TBA	Thiobarbituric acid
TCA	Trichloroacetic acid
TEMED	Tetramethylethylenediamine

LIST OF FIGURES

- Figure 1:** Production of various reactive oxygen species in plant chloroplasts.
- Figure 2:** Production of reactive oxygen species in mitochondria.
- Figure 3:** Production of reactive oxygen species in peroxisomes.
- Figure 4:** Enzymatic and non-enzymatic antioxidant defence mechanisms in plants.
- Figure 5:** Scavenging of ROS by superoxide dismutase and ascorbate peroxidase enzymes.
- Figure 6:** Equilibrium of antioxidants and ROS in plant cells in response to different environmental conditions.
- Figure 7:** Effects of water deprivation on the growth and morphology of Soybean leaves.
- Figure 8:** Changes in shoot lengths of soybean plants in response to drought stress. **Figure 9:** Changes in the number of nodes for soybean plants in response to drought stress. **Figure 10:** Quantification of drought-induced changes in the relative water content of soybean leaves.
- Figure 11:** Measurement of drought-induced changes to the hydrogen peroxide content in Soybean leaves.
- Figure 12:** Measurement of drought-induced changes in lipid peroxidation via detection of malondialdehyde content in soybean leaves.
- Figure 13:** Quantification of the total caspase-like activity in soybean leaves in response to water-deficit.
- Figure 14:** Measurement of the changes in cell death of soybean leaves in response to water-deficit.
- Figure 15:** Analysis of drought-induced changes in the gene expression of Glyma14g04250 and Glyma20g08800 relative to 18S RNA in soybean leaves.
- Figure 16:** Spot densitometry analysis of drought-induced changes in the gene expression of Glyma14g04250 and Glyma20g08800 relative to 18S RNA in Soybean leaves.
- Figure 17:** Real-time Quantitative PCR analysis of the drought-induced changes in gene expression of Glyma14g04250 and Glyma20g08800 in soybean leaves.
- Figure 18:** SDS-PAGE analysis of protein purification by affinity chromatography.
- Figure 19:** Quantification of the inhibitory activities of soybean cystatins Glyma14g04250 and Glyma20g08800.

LIST OF TABLES

Table 1: Full-length primer sets for the PCR amplification and cloning of Glyma14g04250 and Glyma20g08800.

Table 2: Screening of *E.coli* DH5 α transformants for Glyma14g04250 and Glyma20g08800 using Colony PCR.

Table 3: Screening of *E.coli* BL21transformants for Glyma14g04250 and Glyma20g08800 using Colony PCR.

AIMS AND OBJECTIVES OF THE STUDY

- Determine the effects of water-deprivation on soybean growth and development.
- Identify drought-induced changes in soybean plants.
- Quantification of the effects of water-deprivation on the activity of caspase-like enzymes and the resulting changes in cell death.
- Measurement of changes in Glyma14g04250 and Glyma20g08800 expression in response to drought.
- Overexpression, purification and characterization of Glyma14g04250 and Glyma20g08800 via spectrophotometric activity assays.

CHAPTER 1:

LITERATURE REVIEW

1.1. Introduction

Since the evolution of the first terrestrial plants to inhabit the earth approximately 475 million years ago, plants have diversified through the process of evolution and natural selection to form numerous species, adapting in order to thrive in their environment (Fukuyama and Le Bihan 2010). However, since the beginning of time, the ever-present threat faced by plants has been posed by the environment in the form of biotic and abiotic stress factors.

These factors adversely affect plant growth and development, and depending on the severity or duration of the stress, may result in the death of the organism on the whole. Considering how ubiquitous these stresses are in nature, plants have adapted well and employ protective mechanisms to defend themselves against the constant threats of pathogen attack and extreme shifts in environmental conditions (Dangl and Jones 2001). Shifts in environmental conditions may be in an array of forms, but most commonly occur as temperature and water supply extremes.

One of the most prominent stresses affecting plant productivity across the globe can be attributed to conditions of drought. Within a time-frame of approximately 30 years, from 1970 to the year 2000, the percentage of land exposed to conditions of extreme drought increased by more than 2-fold. Periods of drought pose a dangerous threat to both subsistence and commercial crop producers in various agricultural output regions worldwide. Drought in these regions has negative effects on both the crop quality and crop yields achieved, with the most devastating effect being crop failures (Challinor *et al.*, 2010).

This review covers the overall effects and downstream impacts of drought-induced stress in soybean plants on the whole-plant and molecular levels. The focal point centers on the concept of cell death and the regulation of programmed cell death (PCD) in response to drought stress via cystatin and cysteine protease (caspase) interplay.

Drought has a major effect on the total yield of all crop plants worldwide (Tuteja 2007). This is due to the prevalence of drought in many agricultural output regions. In the presence of sufficient water and nutrients, plants develop and grow rapidly, with photosynthesis and metabolism occurring at optimal levels (Letey 1985).

When plants are under conditions where the availability of water is low, plants respond by adapting physical changes to minimize water loss (Gill and Tuteja 2010). These physical changes involve the reduction in the surface area of the leaves to reduce transpiration, build-up of anthocyanins to minimize photosynthetic activity, with closing of the stomata and thickening of cuticles also resulting in a lower rate of water loss (Gill and Tuteja 2010).

Under extended periods of drought, various different physiological changes can be observed at the whole-plant level as well as on the molecular level (Chaves *et al.*, 2003). Changes in phenotype can be seen between plants grown under conditions where there is no deficit in water compared to plants where water availability is low.

Plants grown under drought conditions tend to have their growth stunted and express genes in response to drought stress for survival (Chaves *et al.*, 2003). Depending on the severity and length of the drought, the levels of reactive oxygen species (ROS) within the plant cells increases and build-up (Gill and Tuteja 2010). This accumulation of ROS may lead to oxidative stress, which could be lethal to the plant.

1.2. Reactive Oxygen Species

Reactive oxygen species (ROS) are highly reactive chemical molecules that contain oxygen and are commonly known as oxidants (Apel and Hirt 2004). These ROS come in many different forms, including radical and non-radical forms. The most common radical forms of ROS are superoxide ($O_2^{\cdot-}$), hydroxyl radicals (OH^{\cdot}), perhydroxyl radicals ($HO_2^{\cdot-}$) and the alkoxy radicals (RO^{\cdot}) according to Apel and Hirt (2004). There are various non-radical forms of ROS the most common ones being hydrogen peroxide (H_2O_2) and singlet oxygen (1O_2), but these molecules are equally as significant in signal transduction pathways as well as potential causes of oxidative stress (Gill and Tuteja 2010).

This diversity of ROS molecules is attributed to the fact that oxygen atoms have two unpaired electrons with the same spin quantum number; this spin restriction thus makes oxygen prefer to accept single electrons at a time, forming these reactive radicals (Gill and Tuteja 2010).

1.3. Production of ROS in Plants

UNIVERSITY of the
WESTERN CAPE

Reactive oxygen species are naturally produced in plants through the processes of metabolism, photosynthesis, respiration and many other biochemical processes (Mittler *et al.*, 2004). It is estimated that about 1-2% of the O_2 consumed by plants is used to produce ROS (Puntarulo *et al.*, 1988). The sub-cellular localization of the major sites for ROS production is the organelles which have O_2 present in combination with a high rate of electron flow through their systems (Mittler *et al.*, 2004). Within plant cells, these organelles would correspond to chloroplasts, mitochondria and peroxisomes.

1.3.1. Chloroplasts and ROS Generation

Photosynthesis is the process by which autotrophs capture light and convert the energy into carbohydrates, which are chemical forms of energy (Barker and Carr 1989). In higher autotrophic organisms such as plants, photosynthesis takes place in complex organelles known as chloroplasts (Barker and Carr 1989). These chloroplasts are complex organelles that have highly organized thylakoid membranes which are used as light-capturing systems (Gill and Tuteja 2010).

Two photosystems are responsible for carrying out photosynthesis; P680 (photosystem II) and P700 (photosystem I) as shown in figure 1. Considering that the conditions in chloroplasts are oxygenic due to the oxygen generated from photosynthesis, by proxy it should be known that ROS can thus form from the oxygen accepting electrons flowing through the aforementioned photosystems (Apel and Hirt 2004). This particular ROS would typically be in the form of superoxide radicals according to Apel *et al.*, (2004).

Superoxide radicals are not the only ROS generated within chloroplasts, but are generally the first to be produced (Gill and Tuteja 2010). Singlet oxygen is also typically produced as a by-product of photosynthesis and this ROS production takes place predominantly at photosystem II (figure 1). Following the production of superoxide, on the surface of the stromal membrane; hydrogen peroxide is produced by the dismutation of the superoxide by superoxide dismutase enzymes (Mao *et al.*, 1993).

The production of these ROS depends on the conditions under which a particular plant is grown. Therefore stresses such as biotic and abiotic stresses can result in an increase in the production of ROS in chloroplasts due to overloading of the electron transport chains (ETC's) in photosystems I and II (Gill and Tuteja 2010). The chloroplast is thus a major site for the generation of ROS in plants.

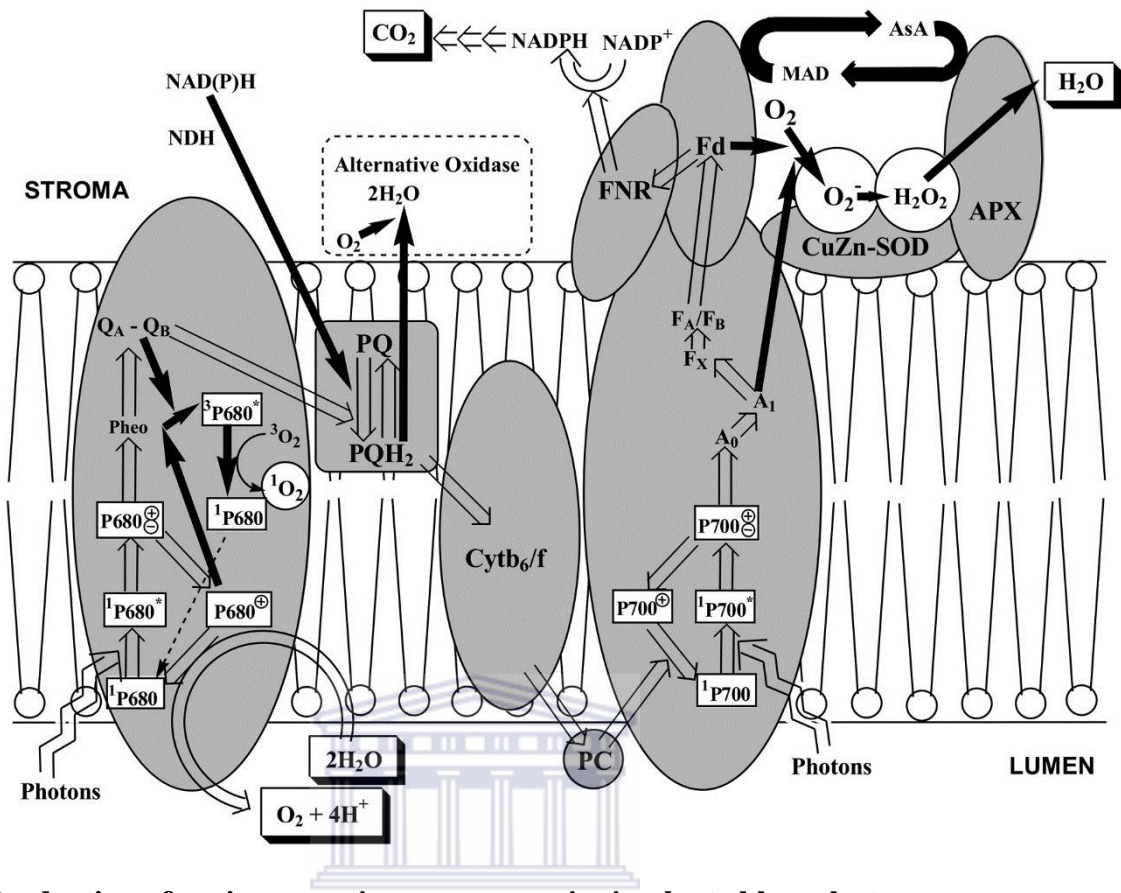


Figure 1: Production of various reactive oxygen species in plant chloroplasts.

Singlet oxygen (${}^1\text{O}_2$) at photosystem II (PS II) and superoxide (O_2^-) as well as hydrogen peroxide (H_2O_2) at photosystem I (PS I). The flow of electrons passing through PS I and II are indicated by grey arrows. However, when the photosystems are overloaded with electrons due to the presence of excess light and insufficient photosynthetic capacity, the electron flow is diverted to generate ROS (shown as black arrows). This figure was adapted from Asada (2006).

1.3.2. Mitochondria and ROS Generation

Mitochondria are the organelles which are majorly responsible for the production of energy in cells for cellular activity and are therefore renowned as the powerhouses of living cells (Loeb, Wallace *et al.*, 2005). The usable energy within cells is found in the form of adenosine triphosphate (ATP) which results from the conversion of carbohydrates by the process of cellular respiration (Loeb, Wallace *et al.*, 2005). Although mitochondria have a conserved function in all living organisms,

mitochondria found in plants differ significantly from those found in other organisms such as animals.

The major difference in plant mitochondria is the additional functionality of photorespiration (Gill and Tuteja 2010). Since photosynthesis takes place in close proximity to the mitochondria within plant cells, this means that the environment surrounding the mitochondria is rich in oxygen and carbohydrates generated by photosynthetic activity (Barker and Carr 1989).

This environment makes a prime site for the production of ROS. Since oxygen is easily available, all that is required to generate ROS is the reduction of the oxygen atoms; which is easily achieved because the electrons present in the ETC have enough free energy to do exactly that (Gill and Tuteja 2010). Subsequently, this process is the primary source for generation of ROS in mitochondria.

Major sites for ROS generation within mitochondria can be localized specifically to complexes I and III in the ETC (figure 2) according to Chen *et al.*, (2003). Superoxide is commonly produced at these sites, which can then be reduced to hydrogen peroxide through dismutation by superoxide dismutase (figure 2). An estimation of between 1-5% of oxygen consumption by mitochondria results in the generation of hydrogen peroxide (Foyer and Noctor 2003).

According to Zepp *et al.*, (1992), hydrogen peroxide may undergo a reaction with reduced iron (Fe^{2+}) or copper (Cu^+) to yield hydroxyl radicals ($\text{OH}\cdot$). These $\text{OH}\cdot$ radicals may diffuse across the mitochondrial membranes and cause damage to lipids through lipid peroxidation.

Even though mitochondria are major producers of ROS, they are also important in adapting to abiotic stress. How this is achieved is through energy-dissipating systems which mitigate production of ROS in the mitochondria (Gill and Tuteja 2010).

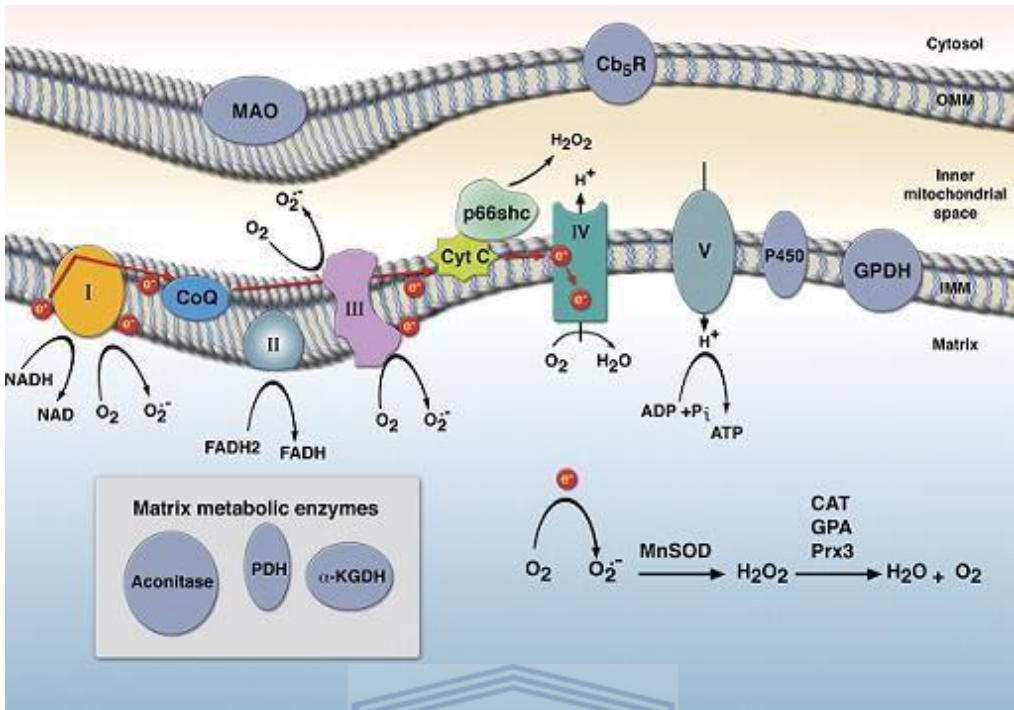


Figure 2: Production of reactive oxygen species in mitochondria. O_2 and H_2O_2 are produced at various sites within a mitochondrion. Complex I and complex III are the major sites for the generation of O_2^- and the major sites for the generation of H_2O_2 are the Mn-SOD in the matrix and p66shc in the inner mitochondrial space. The red arrows in the diagram indicate the flow of electrons through the system from complex I through IV. This figure was adapted from Finkel (2011).

1.3.3. Peroxisomes and ROS Generation

Peroxisomes (also known as microbodies) are relatively small organelles found in almost all eukaryotic cells. These microbodies have a number of functions, but one of its major functions is the catabolism of long chain fatty acids through beta-oxidation.

Due to this type of metabolism, peroxisomes are prone to the production of ROS and are therefore a major contributor to intracellular ROS generation (Møller 2001). The normal metabolism of peroxisomes results in the production of O_2^- radicals (figure 3), which is basically the same as ROS production in chloroplasts and mitochondria.

There are two mechanisms that have been established for ROS production in peroxisomes. One mechanism is specifically localised in the peroxisomal matrix and the other in the peroxisomal membrane. In the peroxisomal matrix, O_2^- is generated by the enzymatic action of xanthine oxidase (XOD) which oxidizes xanthine and hypoxanthine to form uric acid (Corpas *et al.*, 2001) as shown in figure 3. The second mechanism for ROS production also produces O_2^- as a by-product from an ETC (figure 3). The enzyme Monodehydroascorbate reductase (MDHAR) is associated with the production of O_2^- in the peroxisomal membrane (Luis *et al.*, 2002).

Other ROS are also known to be produced in peroxisomes, such as H_2O_2 . Production of H_2O_2 is accredited to a few reactions. These reactions are specifically due to activity of glycolate oxidase and flavin oxidases as well as two other important sources of H_2O_2 production in the various peroxisomes which results from O_2^- disproportionation and beta-oxidation of fatty acids (Huang 1983) as shown in figure 3.

There are many different sites for the production of ROS in plant cells, however; the aforementioned sites produce the majority of the total intracellular ROS.

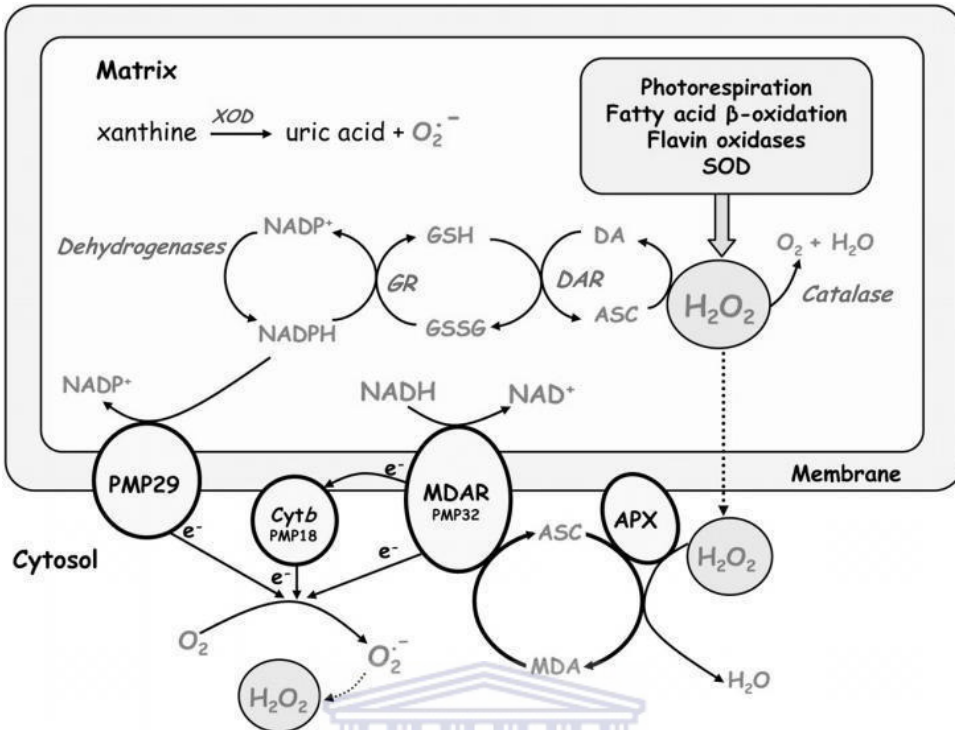


Figure 3: Production of reactive oxygen species in peroxisomes. O_2 and H_2O_2 are generated within both the matrix and cytosol of a peroxisome. O_2 is generated in the matrix via xanthine oxidase activity and free O_2 is reduced to O_2 in the cytosol by accepting electrons from the ETC. H_2O_2 is generated by various reactions in the matrix such as photorespiration, β -oxidation, flavin oxidases and SOD activity. The H_2O_2 pool present in the cytosol is as a result of H_2O_2 diffusion from the matrix as well as generation by disproportionation of O_2^- . This figure was adapted from Rio *et al.*, (2006).

1.4. Significance and Roles of ROS in Plant Signaling and Oxidative Stress

ROS are highly reactive molecules produced as a result of normal metabolism and other biochemical processes (Finkel and Holbrook 2000). These molecules have various roles in plants; however, it is critical that the intracellular concentrations of these ROS are maintained at a constant level. For the survival of plants, it is crucial that intracellular ROS levels are beneath the threshold for toxicity as ROS are known to be toxic molecules (D'Autréaux and Toledano 2007). Therefore depending on the levels of these ROS, they may either be beneficial or detrimental to plants.

At levels below the toxic threshold of plant cells, ROS function as important signaling molecules. This is achieved due to the specificity of O_2^- and H_2O_2 which target specific biomolecules. Both O_2^- and H_2O_2 preferentially target iron-sulphur clusters [Fe-S] because of their atomic reactivity being high (D'Autréaux and Toledano 2007). Where these two ROS differ is that they have separate alternative targets.

1.4.1. Superoxide as a Signaling Molecule

Other than its high affinity for [Fe-S] clusters, O_2^- tends to react with other free radicals such as nitric oxide ($NO\cdot$) and semiquinones (D'Autréaux and Toledano 2007). Despite these attributes, O_2^- is not an ideal molecule for signaling because of a few unfavourable disadvantages. O_2^- is not a very stable molecule as it has an average half-life of 2-4 μs and can easily be disproportionated to H_2O_2 either through spontaneous disproportionation or through SOD-mediated dismutation (Miwa and Brand 2003). Another property of O_2^- that makes its use unfavourable as a signaling molecule is that it is negatively charged, which means that it would not be able to diffuse freely across membranes (Mao and Poznansky 1992).

1.4.2. Hydrogen Peroxide as a Signaling Molecule

The ROS H_2O_2 is actually a relatively weak oxidant in comparison to other ROS (Gutteridge 1995). In terms of targets for biomolecules, other than reacting with [Fe-S] clusters, H_2O_2 also targets certain proteins. These proteins are specifically metallo-enzymes and proteins that have free cysteine (Cys) or methionine (Met) residues which can undergo oxidation by reacting with H_2O_2 (D'Autréaux and Toledano 2007). According to D'Autréaux *et al.*, (2007) the rates of these reactions can be highly variable and is dependent on the protein environment, making the reaction selective and specific. In terms of its properties, H_2O_2 is quite stable and has a half-life of approximately 1 ms as well as a steady intracellular concentration in plants. H_2O_2 also has the ability to diffuse across membranes, making it ideal for use as a signaling molecule (D'Autréaux

and Toledano 2007). However, the cause for concern is when H_2O_2 is reduced to the free radical form HO^\cdot which is highly toxic and reacts indiscriminately with important biomolecules such as lipids, carbohydrates, proteins and nucleic acids (Ohsawa *et al.*, 2007).

Even though it is well-known that at low concentrations, ROS are crucial in plant signaling pathways as secondary messengers; at elevated levels they function as inducers of oxidative stress (Gill and Tuteja 2010).

1.5. ROS Induced Oxidative Stress

When plants are affected by stresses such as biotic or abiotic stresses, the rate of production of ROS is enhanced and thus the intracellular levels of ROS increases (Gill and Tuteja 2010). Once the intracellular levels of ROS exceed the toxic threshold of the plant cells, the cells are in a state of oxidative stress.

On the molecular level, there are three main events which may occur as a result of oxidative stress.

These events are the peroxidation of lipids, oxidation of proteins and ultimately damage to DNA by the introduction of mutations (Wiseman and Halliwell 1996). This particular type of molecular damage is known as oxidative damage.

1.5.1. Lipid Peroxidation (LPO)

Lipids are essential biomolecules that have an array of functions within living organisms, ranging from their structural functionality in organelle and cellular membranes to their central functions in various metabolic pathways (Jones and Papamandjaris 2012). These biomolecules are thus imperative for survival of all living organisms. Considering that lipids are such important biomolecules, molecular damage to lipids is often one of the most destructive events which may occur within cells of living organisms (Gill and Tuteja 2010).

The most common form of molecular damage to lipids is through lipid peroxidation (LPO) by ROS. This type of damage typically occurs when cells are in a state of oxidative stress as a result

of ROS levels exceeding the toxic threshold of the cells. Lipid peroxidation occurs in three stages, specifically defined as initiation, progression and termination (Gill and Tuteja 2010).

The initiation step occurs most commonly by means of a hydrogen atom being abstracted from an unsaturated side chain in a polyunsaturated fatty acid (PUFA) by OH[·]. This results in the formation of a lipid radical, and under aerobic conditions will form a ROO[·] group which can then further react with the side chains of adjacent PUFA's; this is referred to as the progression stage (Gill and Tuteja 2010). Lipid peroxidation is therefore known to be a chain reaction. The termination stage of LPO occurs when either a fatty acid dimer or peroxide bridged dimer forms, resulting in the loss of the reactive radical forms (Gill and Tuteja 2010).

The effects of lipid peroxidation are detrimental to cells as it results in the loss of selective permeability of cellular and sub-cellular membranes due to decreased fluidity, and thus causing leakage (Sharma *et al.*, 2012). These effects may also include damage to important membrane-associated proteins such as receptors and enzymes.

1.5.2. Oxidation of Proteins

Proteins are essentially the main working components of cells and can be broadly categorized into two groups, specifically, structural and functional proteins (Buxbaum 2007). Structural proteins are important in the organization and formation of complexes within cells that aid in cell rigidity and integrity (Buxbaum 2007). Functional proteins on the other hand carry out specific enzymatic reactions or aid in biochemical processes within cells (Buxbaum 2007).

Oxidation of proteins is known as the covalent modification of proteins as a result of reactions with ROS or by-products formed due to oxidative stress (Gill and Tuteja 2010). This particular type of molecular damage is predominantly irreversible modifications to proteins, which may dramatically affect or alter the protein's function on the whole (Gill and Tuteja 2010). However, certain covalent modifications to proteins are known to be reversible, such as the oxidation of sulphur-containing moieties methionine and cysteine (Ghezzi and Bonetto 2003).

The most commonly used indicator of protein oxidation is the degree to which proteins are carbonylated as various amino acids can undergo the process of carbonylation (Møller *et al.*, 2007). However, proteins may also be damaged by reacting with products that have formed from lipids that have undergone peroxidation.

Due to covalent modifications, oxidized proteins may have a loss in function in comparison with the native state proteins (Grimsrud *et al.*, 2008) and therefore these altered functions will in all probability have a negative impact on living cells.

1.5.3. DNA Damage

Deoxyribonucleic acid, more commonly referred to as DNA is the genetic make-up of all living organisms and carries the information containing the codes for millions of proteins essential for life (Lea *et al.*, 2000). Due to the key role of DNA as a carrier of genetic information which is hereditary, damage to DNA such as double stranded breaks is widely regarded as the most devastating type of molecular damage to occur within living cells (Fattah *et al.*, 2010).

The genomes of plants are particularly stable and there are various defence mechanisms in place which prevent the introduction of mutations to the plant genome (Sharma *et al.*, 2012). However, under stressful conditions such as biotic or abiotic stresses, even a plants genome may be damaged due to oxidative stress. DNA damage may then induce further damage by means of genotoxic

stress (Sharma *et al.*, 2012).

ROS are the causative agents for DNA damage as a result of oxidative stress (Hemnnani and Parihar 1998). Specifically, $^1\text{O}_2$ and OH^- are the forms of ROS which induce damage to DNA; whereas O_2^- and H_2O_2 are completely unreactive with nucleic acids (Wiseman and Halliwell 1996). The primary target of attack for $^1\text{O}_2$ is guanine nucleotides, but OH^- molecules are more lethal and can react with all kinds of nucleotides including the sugar-phosphate backbone of nucleic acids (Wiseman and Halliwell 1996).

Damage to DNA may occur in an array of different forms such as deletions, cross-linkages, dimerization of pyrimidines, modifications to bases through oxidation or alkylation, and ultimately may result in strand breaks which fragment DNA (Tuteja *et al.*, 2001). This type of molecular damage can be crippling to plants as protein synthesis is reduced and important proteins and membranes may be damaged which will ultimately affect the growth and development of the entire organism (Britt 1999).

In essence, damage to important biomolecules such as lipids, proteins and nucleic acids may be induced by ROS mediated oxidative stress (Valko *et al.*, 2006). Therefore plants and various other higher organisms have evolved mechanisms to protect themselves against attack by ROS.

1.6. Antioxidant Defence Mechanisms

When plants are exposed to unfavourable conditions such as biotic and abiotic stress, production of intracellular ROS increases (Gill and Tuteja 2010). These ROS may be toxic to the plant cells. If they are allowed to build up to levels exceeding the toxic threshold of the cells (D'Autréaux and Toledano 2007). Plants have therefore evolved protective mechanisms known as antioxidant defence mechanisms which are systems that detoxify or scavenge ROS to levels which are below the toxic threshold of the cells (De Gara *et al.*, 2010). These systems form complex mechanisms

comprised of both enzymatic and non-enzymatic ROS-scavenging pathways (Gill and Tuteja 2010) as shown in figure 4.

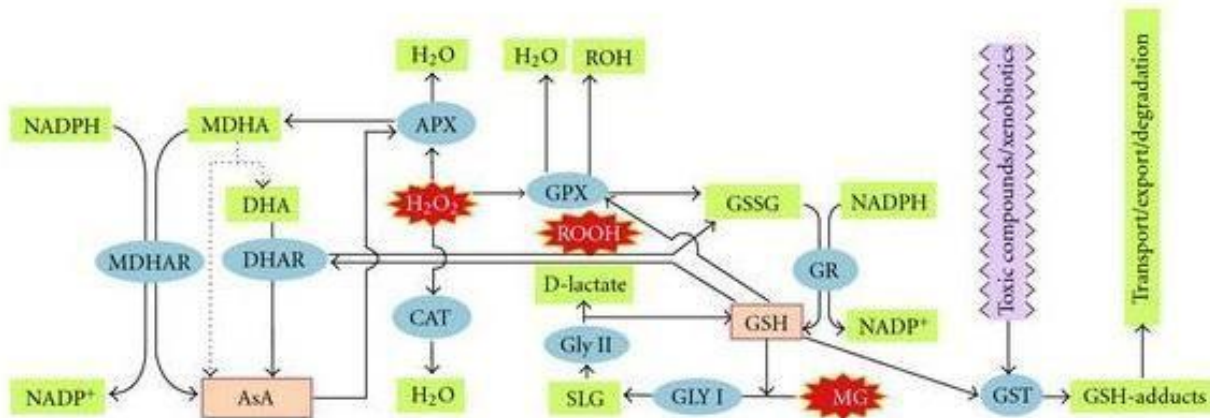


Figure 4: Enzymatic and non-enzymatic antioxidant defence mechanisms in plants.

Interconnected pathways for the detoxification of various ROS. Those indicated in blue are the enzymes involved in the pathways and green indicates the substrates and products of enzymatic activity. Ascorbic acid (AsA) and glutathione (GSH) are indicated as pink as they may scavenge ROS directly or indirectly as substrates in enzymatic reactions. The figure was adapted from Hossain *et al.*, (2011).

1.6.1. Non-Enzymatic Detoxification Pathways

The non-enzymatic mechanisms involve the use of ascorbate (AsA) and glutathione (GSH) as shown in figure 4, as well as tocopherols and carotenoids which all act to mitigate the damaging effects of ROS on plant cells (Gill and Tuteja 2011). The basic concept behind how these molecules aid in preventing oxidative stress is either by directly scavenging ROS or by acting as cofactors or substrates in enzymatic reactions which detoxify ROS (figure 4).

1.6.2. Enzymatic Detoxification Pathways

Various antioxidant enzymes exist within plants in a systematic cycle for the detoxification of ROS (Gill and Tuteja 2010). There are however seven major antioxidant enzymes, namely, superoxide dismutase (SOD), catalase (CAT), ascorbate peroxidase (APX), glutathione peroxidase (GPX), monodehydroascorbate reductase (MDHAR), dehydroascorbate reductase (DHAR) and glutathione reductase (Gill and Tuteja 2010). Although there is equal importance between these seven antioxidants, the main focus in this review will be the significance of SOD and APX antioxidant enzymes.

1.6.2.1. Superoxide Dismutase (SOD)

The metalloenzyme superoxide dismutase catalyzes the dismutation of O_2^- to form H_2O_2 through reduction, and O_2 through oxidation of a second O_2^- molecule (figure 5) according to Gill *et al.*, (2010). The disproportionation of O_2^- to H_2O_2 does occur spontaneously in plant cells, but plants prefer to employ the use of SOD enzymes as the reaction rate is 10000 times faster; this mitigates the production of OH^- through the Haber-Weiss reaction (Gill and Tuteja 2010). SOD enzymes are typically referred to as the first line of defence against attack by ROS as O_2^- is generally the first ROS to be produced in plant cells (Gill and Tuteja 2010).

There are three known isozymes of SOD enzymes and the classification of these SOD enzymes are based on the metal cofactors which they make use of (Gill and Tuteja 2010). The three types of SOD enzymes are the Cu/Zn-SOD (Copper-Zinc SOD), Fe-SOD (Iron SOD) and the Mn-SOD (Manganese SOD). Although these isozymes catalyse the same reaction, their sub-cellular localization differs from one another (Gill and Tuteja 2010).

In plants, the localization of Cu/Zn-SOD is in the cytoplasm, and in higher plants they are associated with the chloroplasts (Luis *et al.*, 2002). The Fe-SOD isozymes are generally not

detected in plants (Ferreira *et al* 2002), but when they are present, they are also found in the chloroplasts of plants according to Alscher *et al.*, (2002). Unlike the aforementioned isozymes, the Mn- SOD isozymes are distributed into two sub-cellular localizations, specifically the peroxisomes and mitochondria in plant cells (del Rio *et al.*, 2003).

The prevalence of SOD enzymes at the aforementioned locations is indicative of the significance of this enzyme in the scavenging of ROS and prevention of oxidative stress. It has also been reported that upregulation of SOD enzymes in response to biotic and abiotic stresses aids in the alleviation of oxidative stress (Gill and Tuteja 2010).

1.6.2.2. Ascorbate Peroxidase (APX)

Ascorbate peroxidases (APX's) are one of the antioxidant enzymes in plants that play a crucial role in the scavenging of ROS. APX's catalyse the reaction for the detoxification of H₂O₂ (Gill and Tuteja 2010) as shown in figure 5. H₂O₂ is produced from superoxide by means of SOD enzymatic activity or through spontaneous dismutation (Gill and Tuteja 2010). This detoxification is achieved by APX's utilizing the substrate ascorbate as an electron donor for the reduction of H₂O₂ to non-toxic molecules, H₂O and O₂, as well as liberating the product dehydroascorbate in the process (Sharma 2012) as shown in figure 5.

There are at least five isoforms of APX's found in plants (Gill and Tuteja 2010). These isoforms have different sub-cellular localization in plant cells. Since chloroplasts are such important organelles in plants, two APX isoforms function within chloroplasts as protection from oxidative damage by H₂O₂; the thylakoid APX (tAPX) and the chloroplast stromal APX (sAPX) (Noctor and Foyer 1998).

There is however cytosolic forms (cAPX) as well as gloxisome membrane forms (gmAPX) found in plants (Noctor and Foyer 1998). It has been well-documented that both SOD and APX's are important antioxidants in plants and are highly involved in the scavenging of ROS in response to

various biotic and abiotic stresses (Gill and Tuteja 2010). Under stressful conditions SOD and APX work in unison for the detoxification of ROS (represented in figure 5).

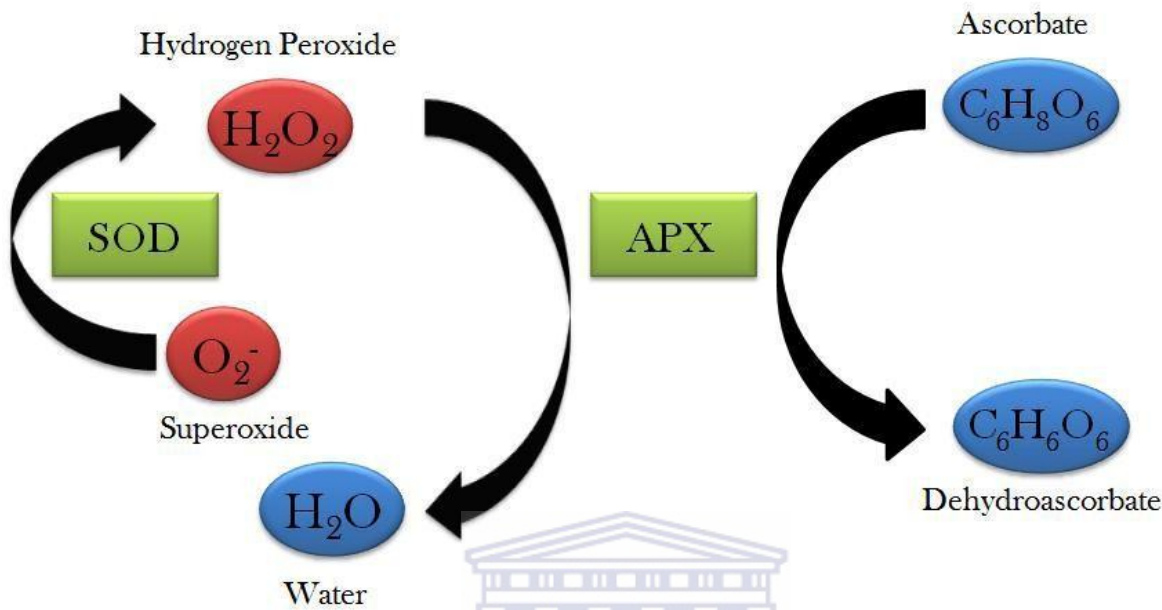


Figure 5: Scavenging of ROS by superoxide dismutase and ascorbate peroxidase enzymes.

Typical detoxification of ROS (shown in red) by superoxide dismutase in combination with ascorbate peroxidase to produce non-toxic molecules (shown in blue). The SOD initially dismutates O_2^- to H_2O_2 and APX ensues to scavenge the H_2O_2 by utilizing ascorbate as a substrate to produce water and dehydroascorbate.

1.7. Regulation of Antioxidants and ROS

The presence of both ROS and antioxidant machinery is vital for the survival of plants in response to various environmental conditions (Choudhury *et al.*, 2013). Under favourable conditions, ROS play important roles as secondary messengers in plant signaling pathways (D'Autréaux and Toledano 2007); but under unfavourable conditions ROS may act as inducers of oxidative stress (Suzuki *et al.*, 2012). Due to this conundrum, plants make use of various antioxidant mechanisms to avoid excess build-up of ROS (Gill and Tuteja 2010).

There is therefore a delicate balance between the levels of ROS and the ROS-scavenging pathways. ROS regulate the expression of antioxidant enzymes and in turn, these enzymes scavenge ROS resulting in equilibrium of oxidants and antioxidants; this is known as ROS homeostasis (Ray *et al.*, 2012).

For optimal functions in plants it is important that the levels of antioxidants and oxidants are kept at equilibrium; ROS generation and ROS-scavenging are equivalent (figure 6). However, ROS build up in response to conditions such as biotic or abiotic stresses, and this increase in intracellular levels of ROS leads to the induction of the antioxidant defence mechanisms in plants for protection from oxidative stress (Limón-Pacheco and Gonsebatt 2009).

The antioxidant defence mechanisms in plants is highly efficient at scavenging ROS, however under extreme conditions where the amount of oxidants produced exceeds the antioxidant capacity, a state of oxidative stress is achieved (Gill and Tuteja 2010) as shown in figure 6. Oxidative stress will result in molecular damage to important biomolecules within cells and eventually lead to cell death (Mullineaux and Baker 2010). Cell death may occur via two different mechanisms in plants, either via the PCD pathway or necrosis.

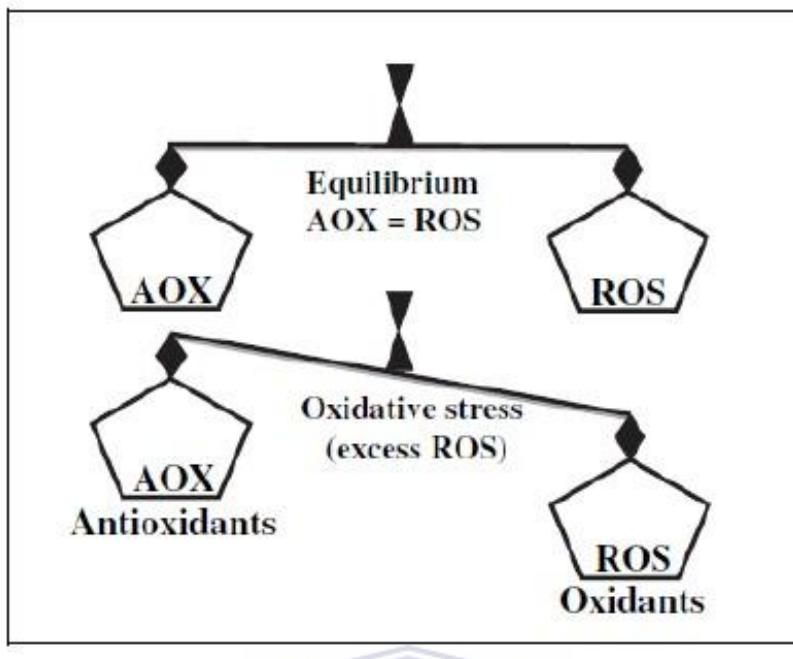


Figure 6: Equilibrium of antioxidants and ROS in plant cells in response to different environmental conditions. Balance between antioxidants and ROS under normal conditions (top) and stressful conditions (bottom). Under conditions devoid of biotic or abiotic stresses, the antioxidants and oxidants will be in equilibrium. However, under stressful conditions, the overproduction and accumulation of ROS induces oxidative stress as it exceeds the antioxidant capacity of the plant cells. The figure was adapted from Gill and Tuteja (2010).

1.8. Programmed cell death and necrosis in plants

Programmed cell death is a naturally occurring phenomenon in all living organisms which plays an invaluable role in maintaining tissue and organs by cell turnover. As cells age in living organisms, they tend to function sub-optimally and therefore need to be replaced by new cells to maintain proper functionality in tissues. This form of cell death is controlled by the organism itself as the organism contains the machinery for the degradation of cells and cellular components (Lodish *et al.*, 2000). Cell death executed by the organism itself is referred to as programmed cell death. The process of cell death in an organism may also be carried out by an uncontrolled mechanism due to infection or wounding. This uncontrolled mechanism of cell death is known as

necrosis (Proskuryakov *et al.*, 2003).

1.8.1. Necrosis in plants

Considering that plants are sessile organisms, they are highly susceptible to damage due to changes in their environmental conditions. External stimuli in the form of biotic and abiotic stressors can easily result in necrosis in plants. Damage to plant tissue may range from high-winds to infection by plant-specific pathogens (Vidaver *et al.*, 2004). Any infection or injury sustained by plants may result in the afflicted tissue undergoing the process of necrotic cell death. Necrosis of the tissue is a common symptom of disease in plants. This form of cell death is uncontrolled and highly volatile, which may have adverse effects on plant growth and development.

1.8.2. Programmed cell death in plants

The controlled turnover of cells in living organisms is carried out by the process of programmed cell death. The programmed cell death pathways vary in different species of organisms. PCD in plants is similar to the process of apoptosis observed in the kingdom animalia (Solomon *et al.*, 1999). Since plants do not possess the ability to incur an immune response, plants have evolved mechanisms such that the PCD pathway induces the production of certain proteins for the degradation of cellular components (Collazo 2006). During the process of PCD in plants, degraded cellular components are transferred into vacuoles before being released into the extracellular space due to dead cells rupturing (Proskuryakov *et al.*, 2003). The components released into the extracellular space do not retain their respective functions as they are degraded during the process of PCD (Beers *et al.*, 2001). The degradation of cellular components is carried out by various proteases; an integral role is executed by cysteine proteases such as caspase-like proteases.

1.9. Cysteine proteases and their roles in the PCD pathways

Proteases are a group of proteins that are specialized in proteolytic degradation by the hydrolysis of peptide bonds in a polypeptide molecule (García-Carreño 1992). Proteases are categorized into groups by discrimination based on their active residues. An example of such proteases is cysteine proteases that incorporate the use of a cysteine residue in their active sites (Oda 2012). This proteolytic activity of cysteine proteases is essential for the controlled and systematic degradation of proteins and cellular components during PCD (Proskuryakov *et al.*, 2003).

Caspases are a group of cysteine proteases that are not only fundamental for the development of cells, but are deeply involved in the modulation of apoptotic PCD in animalia (Hatsugai *et al.*, 2004). Due to the rapid response required for the activation of the caspase signaling cascade, caspases are regulated by post-transcriptional modifications (Ruest 2002). To date, no homologues of caspases have been identified in plants; instead, plants possess proteins which perform similar functions to that of caspases. The plant equivalent of Caspases is therefore called caspase-like proteins (De Jong *et al.*, 2000).

Due to the potentially devastating threat posed by uncontrolled proteolytic activity by caspase-like proteases, plants make use of various cysteine protease inhibitors to modulate caspase-like activity (Danon *et al.*, 2004). Various families of cysteine protease inhibitors have been documented, however; this review focuses on a single family known as cystatins.

1.10. Cystatins and their biological importance in plants

As mentioned above, cystatins are a group of proteins, found in various living organisms, which act as inhibitory agents against cysteine protease activity (Baek and Choi 2008). The main biological targets of cystatins are proteases that belong to the legumain or papain families (Martinez *et al.*, 2007). Cystatin homologues found in plants are more commonly referred to as phytocystatins.

Phytocystatins have been implicated in numerous biological processes ranging from plant defence mechanisms against pathogenic infection, to their involvement in the signaling pathways regulating PCD (Pernas *et al.*, 2000). In plants, cystatins are omnipresent due to their functions in growth and development. Various modes of action have been identified for the inhibition of cysteine proteases by cystatin proteins.

1.11. Mode of action of Cystatins

Cystatins may display inhibitory action against their biological targets by means of at least three unique mechanisms. Through competitive inhibition, cystatins would compete with substrates for access to the active sites of the cysteine proteases (Soares-Costa 2002). By gaining access to the active sites, the cystatins block the access of the substrate to the active residue within the cysteine protease active sites, therefore resulting in inhibition. This process may be a reversible reaction and can ultimately result in substrates out-competing the cystatins as inhibition would be concentration dependent.

Non-competitive inhibition of the cysteine protease activity may alternatively be modulated through allosteric regulation (Habib and Fazili 2007). Cystatins may contain protein domains that are capable of binding their biological targets at an alternative site instead of at the active site. Through this mode of inhibition, cystatins would bind to the cysteine proteases and induce a conformational change of the active site. Due to the conformational change, substrates would no

longer be able to access the active sites of the cysteine protease enzymes.

In addition to these two modes of action, a unique third mode of action has been identified for cystatin-mediated inhibition of cysteine proteases. According to Rzychon *et al.*, (2004) cystatins may act indirectly via backward binding to the cysteine protease substrates instead of to the enzyme itself. Binding of the substrate by cystatins prevent access of the substrates into the cysteine protease active sites, subsequently blocking activity.

1.12. Cysteine proteases, Cystatins and PCD interplay

Due to the importance of cysteine proteases in the process of cell proliferation and PCD, it is essential that these proteins be under tight regulatory mechanisms to ensure optimal functionality. The aspect of PCD in its entirety is overwhelming in its complexity and in equal measure, its importance for the growth and development of living organisms (Jacobson *et al.*, 1997).

As such, under conditions of stress, cysteine protease activity tends to be enhanced and results in the induction of PCD (Mittler 2002). The vital intervention by cystatins is then called upon to regulate cysteine protease activity of caspase-like enzymes in plants in an endeavor to mitigate stress induced PCD (Oliveira *et al.*, 2003). The interplay between caspase-like proteases in plants and their inhibitors are therefore imperative in modulating PCD for the survival of plants in response to various environmental stimuli.

In closing, this study was aimed at the identification of the drought-induced responses of soybean plants to water deficit, particularly focusing on the interplay between soybean cystatins and caspase-like proteases in modulating PCD. The overall aim of this project was to characterize the activities of Glyma14g04250 and Glyma20g08800 as we speculated that upregulation of these two soybean cystatins in transgenic Soybean may confer improved drought tolerance.

CHAPTER 2:

DROUGHT-INDUCED CHANGES IN *GLYCINE MAX* PHYSIOLOGY AND BIOCHEMISTRY AT THE V3 AND R1 DEVELOPMENTAL STAGES

ABSTRACT

Abiotic stressors such as drought have a negative impact on soybean growth and development, which inevitably affects crop productivity. In this study, the effects of drought stress on soybean plants were investigated to determine the molecular level responses of soybean to water deficit. It was found that in response to water deficit, soybean plant leaves contained elevated amounts of H₂O₂ and malondialdehyde content, with a decrease observed in the relative water content of the leaves. Enhancement in the total caspase-like activity and degree of cell death was also shown alongside the differential expression of 3 soybean cystatins in response to water deficit. Gene expression of the three soybean cystatins was measured by semi-quantitative RT-PCR and quantitative real-time PCR analysis. Both sets of gene expression analyses were performed relative to 18S RNA as a reference gene and produced results congruent with one another. Relative gene expression of Glyma14g04250 was observed to be slightly upregulated in response to drought, whilst Glyma20g08800 displayed no changes and Glym18g12240 was not detected in the soybean leaves entirely.

2.1. Introduction

The quality and yields of soybean plants are known to be adversely affected by unfavourable environmental conditions, which threaten their survival (Rai and Takabe 2006). Extreme environmental stimuli may refer to unfavourable environmental conditions due to abiotic or biotic stressors. Abiotic stressors such as drought, salinity and flooding etc. may result in plants experiencing stress (Holmberg and Bülow 1998).

Drought has an array of effects on the growth and development of many species of plants, particularly species which are sensitive to water deficit (Anjum *et al.*, 2011). A lack of sufficient water may manifest effects that can be seen at the whole-plant level, but many of these drought-induced changes may be examined at the molecular level. A typical plant response to drought stress is the accumulation of reactive oxygen species in various cellular compartments such as the mitochondria, peroxisomes and chloroplasts (Mittler *et al.*, 2004).

Under favourable conditions, these molecules are used to mediate signals in the signal transduction pathways, but tend to lead to toxicity at elevated levels (Finkel 2000). A state of oxidative stress sets in when the levels of ROS exceeds the antioxidant capacity of a plant, leading to severe oxidative damage (Gill and Tuteja 2010).

Oxidative stress causes detrimental effects to important biomolecules required for proper cellular function. Oxidative damage in the form of lipid peroxidation and enhanced proteolytic activity of cysteine proteases are particularly alarming. These activities result in the degradation of important proteins, as well as the loss in function due to the degradation of cell and organelle membranes, which ultimately results in cell death (Croft *et al.*, 1990). In this chapter, we aim at elucidating the responses of soybean plants to the effects of water deficit, particularly focusing on the changes occurring at the molecular level.

2.2. Materials and Methods

2.2.1. Germination and growth of *Glycine max*

Soybean seeds were surface-sterilized for 10 minutes in a 10% bleach solution containing 0.35% (v/v) sodium hypochlorite. Following the surface-sterilization, the seeds were rinsed 5 times with distilled water in order to remove the bleach solution. Imbibition of the seeds was then carried out by partial submersion in distilled water for 30 minutes. Once imbibed, the seeds were inoculated with *Bradyrhizobium japonicum* and thorough mixing ensued to ensure that all of the seeds were inoculated.

Soybean seeds inoculated with *Bradyrhizobium japonicum* were placed into wet paper towel and were kept in the dark until germination had occurred. Once the radicles emerged from the seeds, the seeds were then planted into pots containing a 1:1 ratio of compost and potting soil. The pot plants were then supplied with water thrice per week until the Soybean plants reached the V1 developmental stage.

At the V1 developmental stage, the plants were divided into two subsets.

2.2.2. Growth of *Glycine max* until the V3 developmental stage

Continuing from the V1 developmental stage, the first subset of soybeans was grown to the V3 developmental stage before harvesting. The subset was divided into a control and experimental group, containing triplicates of each. The control group was watered regularly whilst water was withheld from the experimental group in order to simulate conditions of drought. The plants were allowed to grow until visible indications of drought stress had set in for the water-deprived soybeans. Harvesting of the soybean leaves occurred at the V3 developmental stage. The third youngest trifoliate leaves were harvested from both the control (well-watered) and experimental

(water-deprived) plants. The harvested leaves were immediately immersed in liquid nitrogen and were ground to a fine powder before storage at -80° C.

2.2.3. Growth of *Glycine max* until the R1 developmental stage

The second subset of Soybean plants were grown up until the R1 developmental stage before harvesting. From the V1 developmental stage, the subset of soybean plants was divided into control and experimental groups. Both groups of plants were watered regularly until the R1 stage of development was achieved. At this stage, the control plants were watered regularly and water was withheld from the experimental plants until visible signs of drought stress had been observed (approximately 3 weeks). The Soybean plants were then harvested.

2.2.4. Measurement of changes in soybean physical parameters

Soybean plants harvested at the R1 developmental stage were measured to determine the differences in their physical parameters as a result of mild drought. The shoot lengths of the plants were measured by using a measuring tape and the number of nodes of each plant were counted for the well-watered and water-deprived plants. Biological replicates were performed in triplicates.

2.2.5. Measurement of drought-induced molecular level changes in soybean at the V3 developmental stage

Changes on the molecular level were quantified by measuring various biochemical markers within the leaf material in order to elucidate the effects of water deficit on the soybean plants. The plant leaf material used for molecular experimentation was obtained from the well-watered and water-deprived plants which were stored at -80° C.

2.2.5.1. Relative water content assay

Measurement of the relative water content within the soybean leaves was determined by weighing the fresh weights of the leaves for the well-watered and water deprived plants, following which, the leaves were then submerged in distilled water for 2 hours. Once complete saturation was achieved, the leaves were weighed for a second time to determine their turgid weights before being incubated at 70° C overnight. The dry weights of the plant leaves were determined the following day and the relative water content was determined mathematically by relating the fresh, turgid and dry weight data to one another.

2.2.5.2. Metabolite extraction (TCA extraction)

In order to determine the hydrogen peroxide content and degree of lipid peroxidation in the soybean leaves, an extraction using trichloroacetic acid was performed. Metabolite extraction was done from the soybean leaves by homogenizing 100mg of the frozen leaf tissue in a 5 times volume (w/v) of 6% TCA. The samples were vortexed vigorously for one minute to ensure complete homogenization. Following the homogenization, the samples were centrifuged at 10000 x g for 20 minutes at 4° C in order to isolate the supernatants from the cellular debris. The TCA extracts were transferred into sterile Eppendorf tubes and were stored at -20° C until further use.

2.2.5.3. Hydrogen peroxide content in soybean leaves

Measurement of the hydrogen peroxide content in the soybean leaves was determined against H₂O₂ standards of known concentrations. The H₂O₂ standard was setup containing known concentrations from 0-5000 nM H₂O₂, 5 mM K₂HPO₄ and 0.25 M KI in a final reaction volume of 200 µl.

Similarly, hydrogen peroxide content in the soybean leaves was measured by mixing 50 µl of the TCA extracts with 5 mM K₂HPO₄ and 0.25 M KI in a final reaction volume of 200 µl. Once the H₂O₂ standard and unknown samples were setup, they were incubated for 10 minutes at room temperature. All reactions were performed in triplicate on a microtitre plate and were measured spectrophotometrically at 390 nm following the incubation period.

2.2.5.4. Lipid peroxidation in soybean leaves

The degree of lipid peroxidation in the soybean leaves was measured indirectly via the quantification of malondialdehyde, a by-product of lipid peroxidation. MDA content was determined by mixing aliquots of the total protein TCA extracts in a 1:2 ratio with a solution containing 20% TCA and 0.5% thiobarbituric acid (TBA) in a final volume of 200 µl. Samples were vortexed briefly for homogenization and were then boiled for 20 minutes at 90° C before a 10 minute incubation step on ice. Experiments were performed in triplicate and were placed on a microtitre plate before absorbances were measured spectrophotometrically at 532 nm and 600 nm.

2.2.5.5. Total caspase-like activity in soybean leaves

To determine cysteine protease activity of caspase-like enzymes in the soybean leaves, total proteins were isolated from the frozen leaf tissue samples. A total of 100mg of leaf tissue was homogenized in a 5 times volume (w/v) of protein extraction buffer (containing 5% glycerol, 10% Polyvinylpolypyrolidone (PVPP) and 100 mM Tris pH 8.0) for both the well-watered and water-deprived samples. Total proteins were isolated from the cellular debris by centrifugation at 10000 x g for 15 minutes at 4° C. Selective inhibition of the threonine and serine proteases within the protein extracts was achieved by the addition of 1 mM Phenylmethylsulfonyl fluoride (PMSF) whilst the addition of 10 mM β-mercaptoethanol reversed the inhibition of cysteine proteases by

PMSF. The samples were then incubated for 5 minutes at 37° C. Following the incubation period, 0.5 mM Caspase-3 substrate (Ac-DEVD-pNA) (Sigma Aldrich) was then added to the samples (containing 50 µg of total protein) before incubation for 60 minutes at 37° C. Total caspase-like activity was measured spectrophotometrically at 405 nm via the detection of p-nitroaniline (extinction coefficient 9.6mM⁻¹.cm⁻¹). Absorbance readings were measured in 10 minute intervals for the duration of the incubation.

2.2.5.6. Cell viability assay for soybean leaves

Cell viability was measured spectrophotometrically via the uptake of Evan's blue dye by the soybean leaves. The degree of dye uptake was inversely proportional to the cell viability (increased uptake is indicative of compromised cellular membrane integrity). Fresh leaves from the well-watered and water-deprived plants were harvested (at V3) and 1 cm²cutlets were excised from the 3rd youngest trifoliolates. The leaf cutlets were individually submerged in 0.25% (w/v) Evan's blue dye for 1 hour to allow maximal dye uptake. After the hour had passed, the leaf cutlets were rinsed thoroughly with distilled water to ensure removal of the excess Evan's blue dye. A 60 minute incubation of the leaf cutlets was then performed in a 1% SDS (w/v) solution at 55° C in order to release the Evan's blue dye into solution. The released Evan's blue dye was detected spectrophotometrically by measuring the absorbance readings at 600 nm for each triplicate sample. Cell viability was measured as an inverse function of Evan's blue uptake. Technical and biological replicates were performed in triplicate.

2.2.5.7. Analysis of Glyma14g04250, Glyma18g12240 and Glyma20g08800 gene expression

2.2.5.7.1. Extraction of total RNA from soybean leaves

Total RNA was extracted from soybean leaves for both well-watered and water-deprived samples using the Direct-zolTM RNA Miniprep kit (Zymo Research). Samples were prepared by homogenizing 50 mg of soybean leaf material in a 10 times volume of TRI REAGENT®. Homogenization was performed by vortexing samples at room temperature for 1 minute to facilitate chemical lysis of the plant cells. Cellular debris was removed from the samples via centrifugation at 10 000 x g for 2 minutes at 4° C. Supernatants obtained from centrifugation were transferred to sterile RNase-free tubes and were mixed with an equal volume of absolute ethanol (>98%) by vortexing thoroughly. The mixtures were then transferred into Zymo-spinTM IIC columns and were centrifuged for 1 minute at 10 000 x g. A prewash step was then performed on the RNA bound to the Zymo-spinTM IIC columns by the addition of Direct-zolTM RNA PreWash, followed by centrifugation for 1 minute at 10 000 x g. A second prewash step was carried out in the same manner prior to the total RNA wash step. The RNA wash was performed by the addition of RNA Wash Buffer to the Zymo-spinTM IIC columns, followed by centrifugation at 10 000 x g for 1 minute. Prior to the elution of the total RNA, a centrifugation step was performed at 10 000 xg for 2 minutes in order to dry the column membranes and to facilitate the removal of excess wash buffer. The total RNA was then eluted from the Zymo-spinTM IIC columns in a final centrifugation step. Elution of the total RNA was performed by the addition of nuclease-free water, followed by centrifugation at 13 000 x g for 1 minute. Prior to the storage of the total RNA samples at -20° C, 40 U of RibolockTM (Thermo Scientific) was added to the samples to prevent RNA

degradation. RNA concentration and purity was determined by using a NanoDropTM 1000 spectrophotometer (Thermo Scientific).

2.2.5.7.2. DNase treatment of total RNA samples

Total RNA extracted from the soybean leaf material was subjected to a DNase treatment reaction to facilitate the degradation of contaminating DNA. DNase treatment was performed on aliquots of the total RNA samples. A total of 1 µg of RNA was subjected to DNase treatment in a reaction containing 2 U DNase I (New England Biolabs), 40 U RibolockTM (Thermo Scientific) in a 1X DNase I Reaction Buffer (New England Biolabs) made up to a final reaction volume of 30 µl with nuclease-free water. Following the setup, the reactions were incubated for 30 minutes at 37° C. Upon completion of the reaction, the DNase was heat inactivated by incubation for 5 minutes at 65° C in the presence of 0.5 mM EDTA. The RNA samples were then stored at -20° C for further use. RNA concentration and purity was determined by using a NanoDropTM 1000 spectrophotometer (Thermo Scientific).

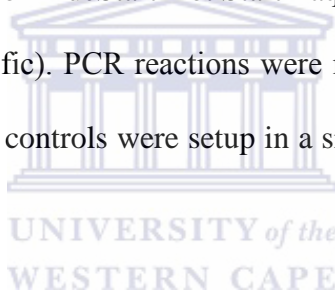
2.2.5.7.3. First strand cDNA synthesis from Dnase-treated RNA samples

First strand cDNA synthesis was carried out by using the first strand cDNA synthesis kit (Thermo Scientific). The reaction setup consisted of 300 ng of template RNA, 15 pmol Oligo dT primers, 1 mM dNTPs, 20 U RibolockTM and 200 U of RevertAid in a 1X reaction buffer. Following the reaction setup, the cDNA synthesis reactions were incubated at 42° C for an hour. Upon completion of the incubation period, the reactions were terminated via heat inactivation at 80° C for 5 minutes. The samples were then stored at -20° C for further use.

2.2.5.7.4. Semi-quantitative PCR analysis of gene expression for Glyma14g04250, Glyma18g12240 and Glyma20g08800 relative to 18S RNA

In order to analyse gene expression of the three soybean cystatins genes via the polymerase chain reaction, the PCR parameters needed to be optimized for optimal amplification of each gene. A temperature gradient of 56°-66° C was used to determine the optimal annealing temperature for each gene.

The PCR setup per reaction consisted of 20 µg template cDNA, 0.4 µM of forward and reverse primers, 200 nM dNTPs and 0.5 U of TrueStart Hot Start Taq polymerase in a 1X reaction buffer containing MgCl₂ (Thermo Scientific). PCR reactions were made up to a final volume of 25 µl with nuclease-free water. Negative controls were setup in a similar manner, with the omission of template DNA.



Temperature parameters and time frames used for the PCR reactions were executed as follows. Initial denaturation was performed at 95° C for 2 minutes, followed by 30 cycles of denaturation at 95° C for 30s, annealing at 56° C for 30s and extension at 72° C for 60s. Final extension was performed at 72° C for 7 minutes to ensure the completion of the PCR reactions. Glyma14g04250 and Glyma20g08800 were amplified optimally at T_A= 56° C whilst 18S RNA was amplified separately at T_A= 58° C.

Following the successful PCR amplification of the target and reference genes from the well-watered and water-deprived samples, gene expression was analysed via agarose gel electrophoresis. PCR products were subjected to gel electrophoresis on a 1% agarose gel for 45 minutes at 90V in the presence of GelRed™ (Biotium) visualizing agent. The PCR products were

visualized by UV translumination and were analysed by spot densitometry using AlphaEaseFC™ software (Version 4.0.0). Gene expression patterns of Glyma14g04250, Glyma18g12240 and Glyma20g08800 were measured relative to 18S RNA.

2.2.5.7.5. Quantitative real-time PCR analysis of Glyma14g04250, Glyma18g12240 and Glyma20g08800 gene expression

Gene expression patterns of Glyma14g04250, Glyma18g12240 and Glyma20g08800 observed using RT-PCR were confirmed and measured through quantitative real-time PCR. 18S RNA was used as reference genes in order to determine the relative gene expression of the 3 soybean cystatins. The qPCR reaction setup for each sample constituted 10 µg template cDNA, 0.3 µM of forward and reverse primers made up to a final volume of 10 µl with SYBR green mastermix and nuclease-free water. Negative controls were setup in a similar manner, with the omission of template DNA. The temperature parameters for the qPCR consisted of an initial denaturation step of 95° C for 2 minutes, followed by 50 cycles of denaturation at 95° C for 30s, annealing at 55° C for 30s and extension at 72° C for 60s. A final extension step was performed at 72° C for 5 minutes. qPCR reactions were setup in triplicate for all target and reference genes with PCR efficiencies determined by performing qPCR standards of elongation factor 2b. The qPCRs were performed and analyzed on a LightCycler® 480 II instrument.

2.3. Results

2.3.1. Drought-induced changes in soybean leaf morphology

Water is arguably the most fundamental biomolecule needed to sustain the life of living organisms. Due to the omnipresence of water molecules playing key roles throughout biological systems, the importance of a molecule as simple as water does not go unnoticed. Plants in particular are extremely dependent and highly affected by water availability. It has been well documented that water deprivation has an array of effects on plants.

Some of these effects may be visible to the naked eye at the whole-plant level as seen in figure 7.

As shown below (figure 7), a comparison between leaf trifoliates of well-watered soybean plants and water-deprived soybean plants revealed various key differences in response to desiccation. With regular watering, well-watered plants showed a higher degree of growth and development with no physical signs of retardation. In comparison, the water-deprived plants showed signs to the contrary.

Growth and development of the water-deprived plants seemed to have been stunted in response to water deficit. The leaf trifoliolate of the water-deprived plant showed significant signs of drought stress, indicative of severe desiccation. Amongst these signs were two vital indicators of desiccation, with the first being a change in the leaf morphology and the second, a change in pigmentation.

These changes in particular are known to be a defence mechanism for plants to minimize photosynthetic activity within the leaves by lowering their total surface area and accumulating anthocyanins (Nielson *et al.*, 2011). These effects are typically brought on by detrimental environmental stimuli causing an excess build-up of reactive oxygen species in the plants, inducing a state of oxidative stress. In this experiment, it was clearly observed that a severe lack of sufficient

water resulted in a drought- induced state of oxidative stress for the water-deprived plants (Figure 7).

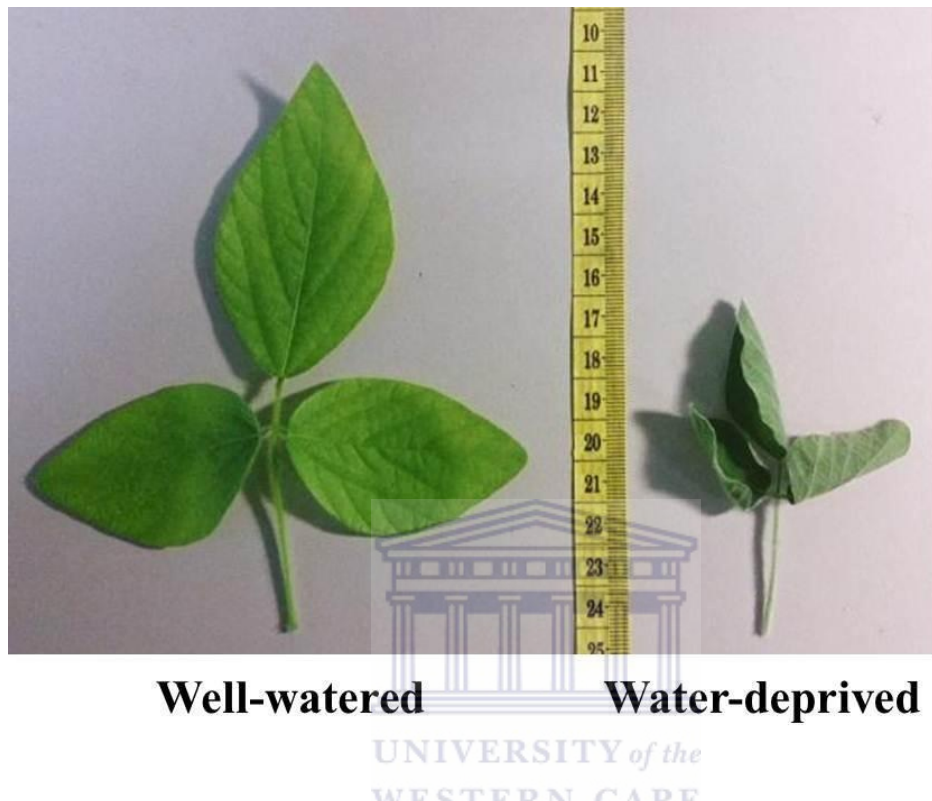


Figure 7: Effects of water deprivation on the growth and morphology of Soybean leaves.

Trifoliate leaves harvested from well-watered (WW) and water-deprived (WD) soybean plants at the V3 developmental stage. Leaves from the well-watered soybeans displayed a higher degree of growth compared to the stunted growth of the water-deprived plant leaves. Changes in pigmentation and leaf curling were also observed in response to water deficit.

2.3.2. Measurement of changes in soybean physical parameters

The effects of drought on the growth and development of soybean plants during their reproductive stages (R1) was tested to determine if any significant changes occur to the physical parameters of the soybean plants. In particular, the experiment was focused at possible drought-induced changes to the shoot lengths and number of nodes developed during plant growth under simulated drought.

2.3.2.1. Changes in shoot lengths for soybean plants in response to drought stress

Interestingly, the results obtained from the experiment suggested that no statistically significant changes in the shoot lengths were observed (figure 8). At the point of harvesting, the R1 developmental stage, both the well-watered and water-deprived plants had shoot lengths in excess of 1 metre. Upon statistical analysis using ANOVA, it was observed that there were no significant differences in the shoot lengths for the well-watered and water-deprived plants in response to water deficit. This result indicated that exposure of soybean plants to water deprivation for a period of 3 weeks did not significantly retard plant growth.

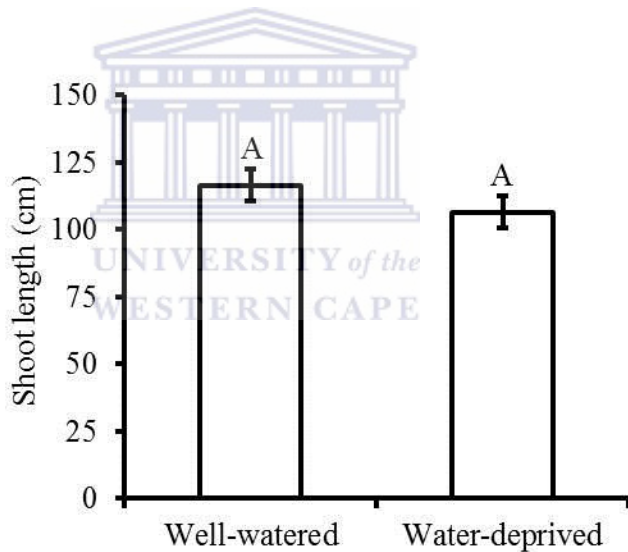


Figure 8: Changes in shoot lengths of Soybean plants in response to drought stress. Soybean plants were harvested at the R1 developmental stage after 3 weeks of water-deprivation for a subset of the plants. The well-watered plants were watered thrice per week for the duration of the experiment while water was withheld from the water-deprived plants. Statistically, no significant changes were observed for the shoot lengths in response to water-deficit. Error bars were generated using the means \pm standard error for 3 independent experiments.

2.3.2.2. Changes in number of stem nodes for soybean plants in response to drought stress

Similarly to the results obtained for the shoot lengths, no significant changes were observed for the number of stem nodes formed during the growth and development of well-watered and water-deprived soybean plants. As shown in figure 9, both well-watered and water-deprived plants had a total average of 10 stem nodes per plant.

This result indicated that a 3 week exposure to water deficit for soybean plants transitioning into the R1 developmental stage had no overall effect on the number of stem nodes developed.

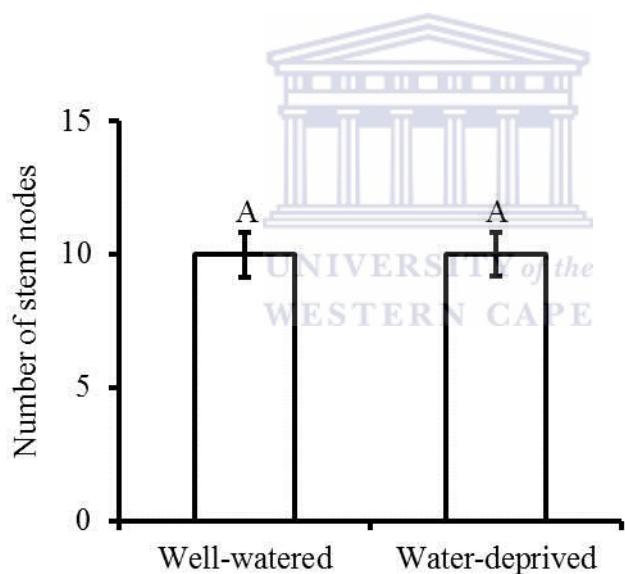


Figure 9: Changes in the number of nodes for Soybean plants in response to drought stress.

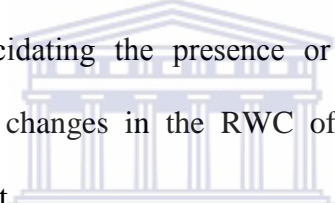
Soybean plants were harvested at the R1 developmental stage after 3 weeks of water-deprivation for a subset of the plants. The well-watered plants were watered thrice per week for the duration of the experiment while water was withheld from the water-deprived plants. Statistically, no significant changes were observed for the number of nodes in response to water-deficit. Error bars were generated using the means \pm standard error for three independent experiments.

2.3.3. Measurement of drought-induced molecular level changes in soybean

Even though water deprivation had not yielded significant changes on the physical parameters of the soybean plants at the whole-plant level, subtle differences on the molecular level might have been detected. As such, various experiments were performed to shed light on the effects of water-deprivation on the molecular level changes observed during plant drought responses.

2.3.3.1. Quantification of drought-induced changes in the relative water content of soybean leaves

The relative water content of plant leaves and roots tend to be useful indicators of a plant's water status. Determining the relative water content of the former organ rather than the latter is more commonly used method for elucidating the presence or absence of water in the plant's environment. In this experiment, changes in the RWC of the soybean plant leaves were a significant indicator of water deficit.



As displayed in figure 10, a 30% decline in the leaf relative water content was observed in response to water deficit. The leaves of the well-watered plants showed a RWC of 90% compared to the 60% observed for the water-deprived plant leaves. The relative water content recorded for the well-watered plant leaves was close to the maximum capacity (100%) whereas the water-deprived plant leaves were 40% adrift from the maximum capacity.

This vast difference in the leaf RWC suggested that the water-deprived plants were exposed to water deficit for long enough to simulate conditions of drought and therefore have experienced drought stress.

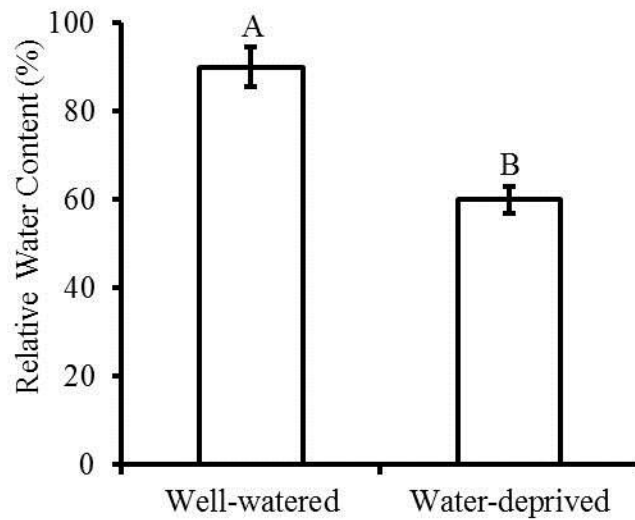


Figure 10: Quantification of drought-induced changes in the relative water content of soybean leaves. Soybean plant leaves were harvested at the V3 developmental stage for well-watered and water-deprived plants. At the V1 developmental stage, well-watered plants were watered thrice per week while water was withheld from the water-deprived plants until harvest. A significant drop (of approximately 30%) in the leaf relative water content was observed in response to water-deficit. Error bars were generated using the means \pm standard error for three independent experiments.

2.3.3.2. Measurement of drought-induced changes in hydrogen peroxide content in soybean leaves

The results shown in figures 7 and 10 clearly indicated that conditions of simulated drought had been achieved by the experimental design. Additionally, the changes in leaf morphology and pigmentation (figure 7) in response to the water deficit strongly suggested that the plants had been experiencing these detrimental effects due to drought stress. Further investigation into the effects of drought stress was carried out to determine the severity thereof and to ascertain whether the plants had been experiencing oxidative stress. Hydrogen peroxide content of the soybean leaves was measured in response to drought as elevated levels of H_2O_2 content is usually an indicator of

oxidative stress.

In response to drought stress, it was observed that H₂O₂ levels had in fact been elevated quite significantly (figure 11). As shown in figure 11, the H₂O₂ content obtained for the well-watered plants corresponded to approximately 0.6±0.05 µmol.mg⁻¹ FW which increased to about 0.9±0.05 µmol.mg⁻¹ FW for the water-deprived plant leaves. Overall, an estimated 67% increase in hydrogen peroxide content was observed in the soybean leaves in response to water deficit, which highly suggested a state of oxidative stress was in effect.

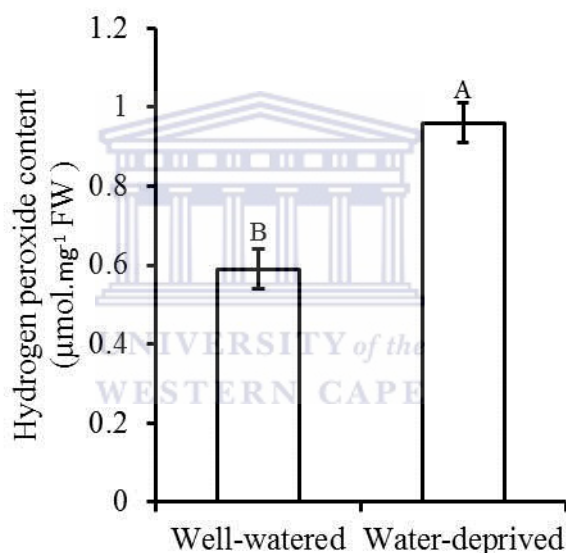


Figure 11: Measurement of drought-induced changes to the hydrogen peroxide content in soybean leaves. Hydrogen peroxide content was measured in soybean leaves for well-watered and water-deprived plants harvested at the V3 developmental stage. It was observed that in response to water-deficit, hydrogen peroxide content in the leaf tissue increased greatly. Error bars were generated using the means ± standard error for three independent experiments.

2.3.3.3. Measurement of drought-induced changes in lipid peroxidation via detection of malondialdehyde content in soybean leaves

In addition to the measurement of hydrogen peroxide content as a primary indicator of oxidative stress, lipid peroxidation was measured via the detection of malondialdehyde in soybean leaves as a secondary indicator for oxidative damage.

As shown in figure 12, a dramatic increase in the MDA content of soybean leaves was observed in response to water deficit. The MDA levels for the soybean leaves of well-watered plants equated to 0.05 ± 0.0045 nmol.mg⁻¹FW, which was met by a dramatic 4-fold rise in MDA content for the water-deprived soybean plant's leaves. The MDA content for water-deprived plants was approximately 0.2 ± 0.0045 nmol.mg⁻¹FW.

As a result, the degree of lipid peroxidation confirmed that the water-deprived plants had been experiencing severe oxidative damage.

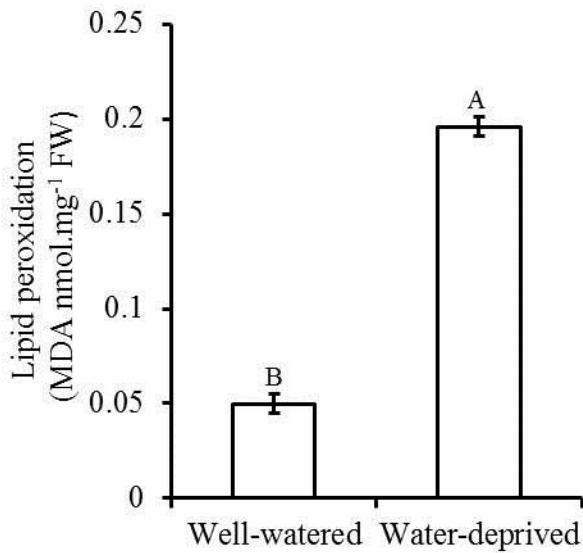


Figure 12: Measurement of drought-induced changes in lipid peroxidation via detection of malondialdehyde content in soybean leaves. MDA content was measured in soybean leaves for well-watered and water-deprived plants harvested at the V3 developmental stage. An approximate 4-fold increase in the MDA content of Soybean leaves was observed in response to water-deficit. Error bars were generated using the means \pm standard error for three independent experiments.

UNIVERSITY of the
WESTERN CAPE

2.3.3.4. Quantification of total caspase-like activity in soybean leaves in response to water-deficit

Caspase-like enzymes in plants play an integral role in modulating cell death by influencing the programmed cell death pathway. Total caspase-like activity was measured in the leaves of soybean plants which were well-watered in comparison to water-deprived plants (figure 13).

It was observed that for the well-watered and water-deprived plants, the total caspase-like activity detected in the leaf tissue was estimated at $16 \pm 4 \text{ } \mu\text{mol}.\text{min}.\text{mg}^{-1} \text{ FW}$ and $44 \pm 4 \text{ } \mu\text{mol}.\text{min}.\text{mg}^{-1} \text{ FW}$ respectively. In essence, it was seen that the total caspase-like activity in soybean leaves was upregulated 3-fold in response to water deficit. This was indicative that the level of cell death experienced by the water-deprived plants increased significantly.

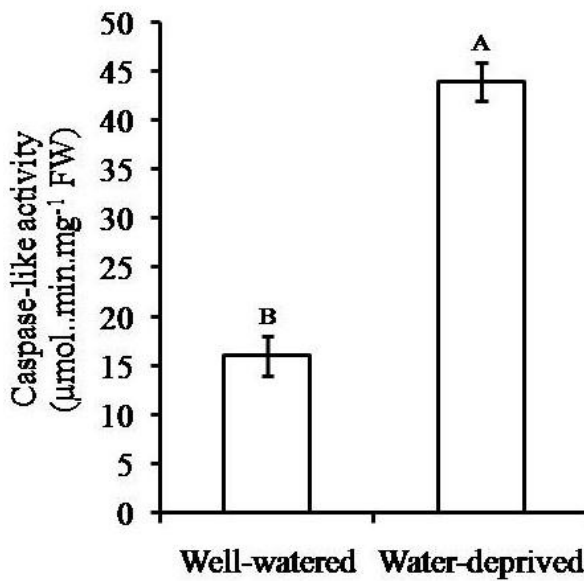


Figure 13: Quantification of the total caspase-like activity in Soybean leaves in response to water-deficit. Total caspase-like activity was measured in Soybean leaves for well-watered and water-deprived plants harvested at the V3 developmental stage. An approximate 3-fold increase in the total caspase-like activity of the soybean leaves was observed in response to water-deficit. Error bars were generated using the means \pm standard error for three independent experiments.

UNIVERSITY of the
WESTERN CAPE

2.3.3.5. Measurement of the changes in cell death of soybean leaves in response to water-deficit

The effects of ROS accumulation typically have a domino effect on various processes in plant cells. An example of this was seen in the aforementioned results as a simple increase in H₂O₂ content led to a dramatic increase in lipid peroxidation, and in combination with elevated activities of caspase-like enzymes, these downstream effects ultimately result in cell death. In this experiment, the degree of cell death was measured in order to determine the effects of water deficit on cell death in soybean plant leaves. Cell death was measured in the leaves of soybean plants for well-watered and water-deprived plants. It was found that the levels of cell death was increased by approximately 3-fold in response to water deficit (Figure 14).

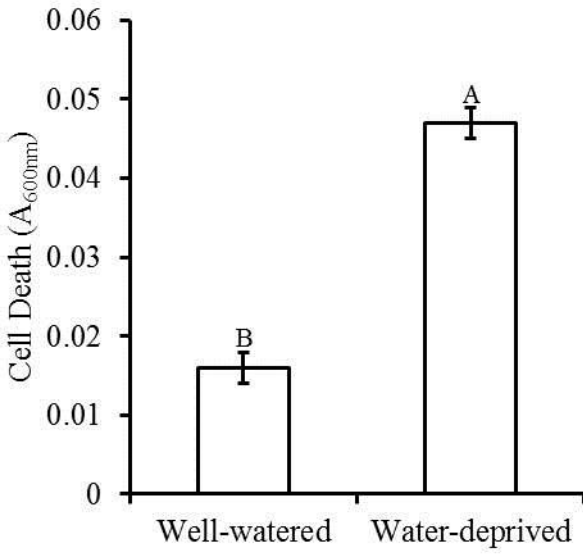


Figure 14: Measurement of the changes in cell death of soybean leaves in response to water-deficit. Cell death was measured in Soybean leaves for well-watered and water-deprived plants harvested at the V3 developmental stage. An approximate 3-fold increase in the cell death of the Soybean leaves was observed in response to water-deficit. Error bars were generated using the means \pm standard error for three independent experiments.

2.3.3.6. Analysis of drought-induced changes in relative gene expression of Glyma14g04250, Glyma18g12240 and Glyma20g08800 via semi-quantitative RT-PCR

In order to analyse the effect of water deficit on the gene expression patterns of Glyma14g04250, Glyma18g12240 and Glyma20g08800, semi-quantitative RT-PCR was performed to amplify all three cystatin genes, as well as 18S RNA for use as a reference gene. Prior to statistical analyses using ANOVA, upon observation, it was determined that only two cystatin genes, namely, Glyma14g04250 and Glyma20g08800 were expressed in the soybean leaves (Figure 15).

Glyma18g12240 was not detected in the leaves, indicating that it was not expressed. Although, it

was observed that drought resulted in slight upregulation in gene expression of Glyma14g04250 whilst Glyma20g08800 remained unchanged. The negative controls showed no amplification, indicating that the actual amplicons obtained for the PCRs corresponded to the target genes. Spot densitometry was then utilized to determine the level of gene expression of the target genes relative to 18S RNA (Figure 16).

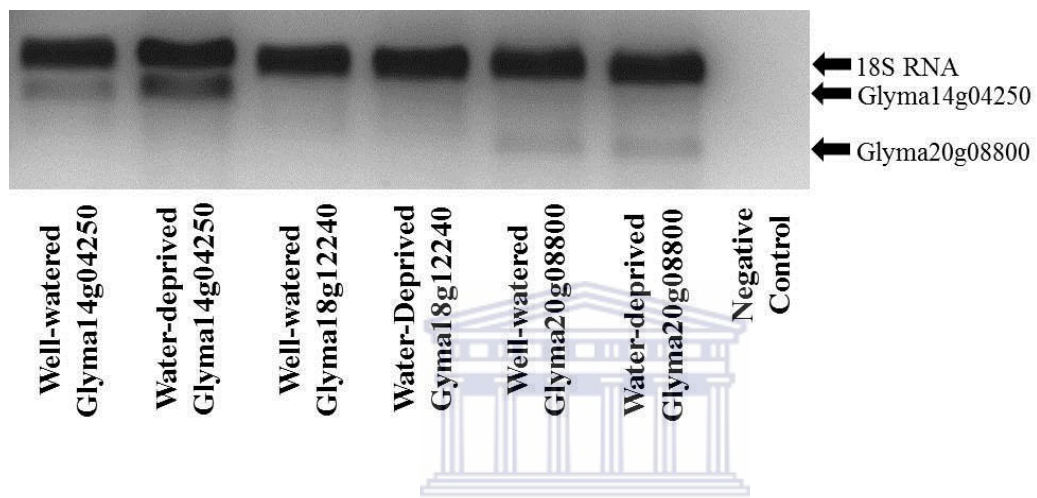


Figure 15: Analysis of drought-induced changes in the gene expression of Glyma14g04250 and Glyma20g08800 relative to 18S RNA in soybean leaves. Gene expression patterns of Glyma14g04250 and Glyma20g08800 were measured via semi-quantitative PCR. Glyma14g04250 and Glyma20g08800 were amplified using gene-specific primer sets to amplify fragments of the full-length genes. Fragments were analyzed by gel electrophoresis on a 1% agarose gel. It was observed that gene expression for both Glyma14g04250 and Glyma20g08800 were upregulated in response to drought.

Results obtained from the statistical analyses of the target gene expression were congruent with the abovementioned observations. Statistical analysis using ANOVA showed that Glyma14g04250 was slightly up-regulated (~30% up-regulation) in response to water deficit whilst no changes in the relative gene expression of Glyma20g08800 were observed (figure 16). Under well-watered conditions, it was shown that the relative gene expression levels of both cystatin genes were statistically identical.

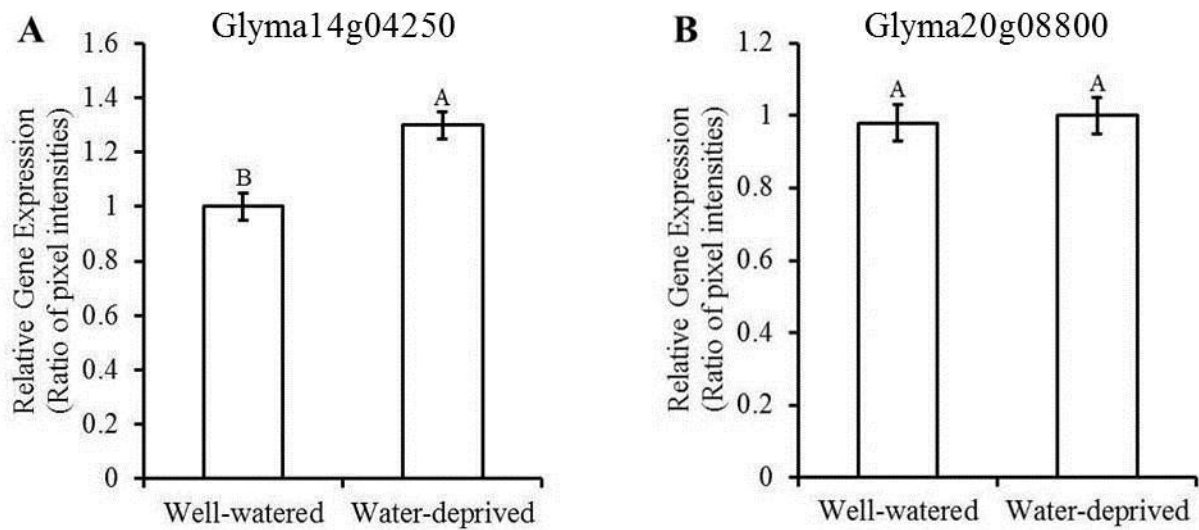


Figure 16: Spot densitometry analysis of drought-induced changes in the gene expression of Glyma14g04250 and Glyma20g08800 relative to 18S RNA in soybean leaves. The graph above depicts the gene expression patterns of Glyma14g04250 (A) and Glyma20g08800 (B) obtained via semi-quantitative PCR and was quantified using spot densitometry. The relative gene expression of Glyma14g04250 (A) was shown to increase slightly in response to water-deficit, whereas Glyma20g08800 (B) remained unchanged under the same conditions. Error bars were generated using the means \pm standard error for three independent experiments.

2.3.3.7. Real-time analysis of drought-induced changes in relative gene expression for Glyma14g04250 and Glyma20g08800 via qPCR

The relative gene expression pattern trends for Glyma14g04250 and Glyma20g08800 observed above (figures 15 and 16) were confirmed using quantitative real-time PCR analysis (figure 17). Using qPCR, it was observed that the relative gene expression for Glyma14g04250 was up-regulated in response to water deficit whilst Glyma20g08800 remained unchanged. Overall, the same trends were observed for the gene expression patterns of Glyma14g04250 and Glyma20g08800 whether using semi-quantitative RT-PCR or quantitative real-time PCR.

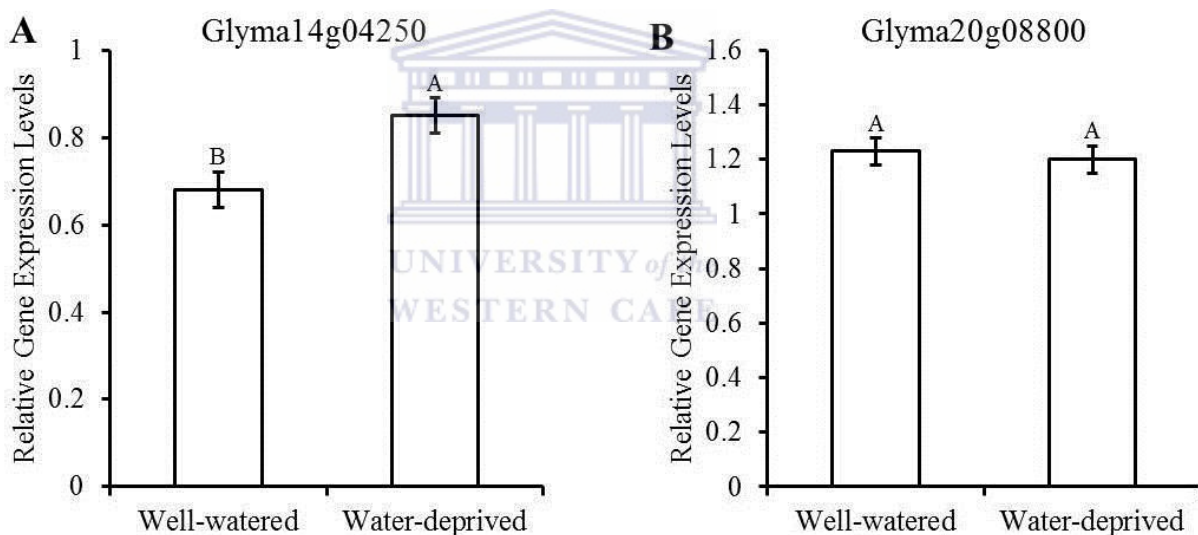


Figure 17: Real-time Quantitative PCR analysis of the drought-induced changes in gene expression of Glyma14g04250 and Glyma20g08800 in soybean leaves. Gene expression of Glyma14g04250 and Glyma20g08800 was measured relative to 18S RNA. It was shown that the relative gene expression levels of Glyma14g04250 (A) were enhanced slightly in response to water-deficit, whereas Glyma20g08800 (B) remained unchanged under the same conditions. PCR efficiencies were determined to be approximately 2. Error bars were generated using the means \pm standard error for three independent experiments.

2.4. Discussion

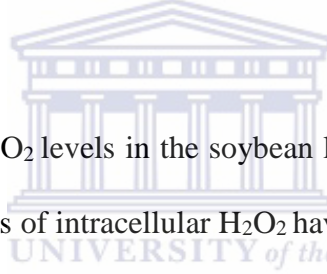
This chapter of the study was focused on elucidating the effects that drought stress imposed on the growth and development of soybean plants. Interestingly, the 3 week exposure of soybean plants (harvested at the R1 developmental stage) to water deprivation had no significant effect on the shoot lengths and number of stem nodes. A similar study performed by Ashraf *et al.*, (2005) on two leguminous species of plants showed that drought manifested a decline in shoot lengths and mass.

This result could have been due to the fact that the evaporation rates of the water from the soil were not quick enough to simulate conditions of drought in this study. In essence, the soybean plants were not deprived of water for a sufficient period of time in order to observe drought-induced changes to their physical parameters. However, the results generated for the plants exposed to water deficit at the V3 developmental stage displayed major changes, some visible at the whole-plant level and others at the molecular level.

The first results observed dealt with the visible changes to the plant leaf morphology and pigmentation in response to water deficit. Clear signs of drought had been observed for the plants that were deprived of water. Retarded development and curling of the leaves were indicators of severe drought stress for the water-deprived plants. In combination with leaf curling, changes in the pigmentation of the leaves were also observed which is generally attributed to accumulation of anthocyanins. It has been well established that the accumulation of anthocyanins is a defence mechanism that many plant species employ to prevent photoinhibition (Steyn *et al.*, 2002). These major changes to the soybean plant leaf morphology was a significant indicator of the plants experiencing drought stress, which was then confirmed by further molecular analyses.

The relative water content of soybean leaves were measured as a molecular indicator of drought. Well-watered soybean plants had a relative water content of 90% in their leaves, compared to the 60% recorder for the water-deprived plants. A 30% drop in the relative water content of the water-deprived plants in comparison to that of the well-watered plants was observed. This trend was observed by Keyvan (2010) in a similar study with wheat plants.

This drop in the RWC of the soybean leaves confirmed that the water-deprived plants were exposed to severe conditions of drought. Drought stress typically leads to the accumulation of ROS such as superoxide and hydrogen peroxide. Excess amounts of these ROS may have detrimental effects on plants as ROS at elevated levels tend to be toxic and may lead to oxidative damage (Gill and Tuteja 2010).



In this study, it was shown that H_2O_2 levels in the soybean leaves were elevated significantly in response to drought. Elevated levels of intracellular H_2O_2 have been implicated in membrane and organelle damage due to their direct roles in the peroxidation of lipids. As expected, the degree of lipid peroxidation in the leaves of water-deprived plants was astronomically high in comparison to that of the well-watered plants. This was congruent with findings by Irigoyen *et al* (1992) in a drought experiment where it was found that water deficit induced lipid peroxidation.

A 4-fold increase in MDA content was most likely due to the downstream effect of the elevated levels of H_2O_2 in the water-deprived Soybean leaves. This high degree of lipid peroxidation was expected to play a major role in the degree of cell death experienced by the water-deprived plants.

The detrimental effects of lipid peroxidation should have contributed significantly to the degree of cell death, considering that peroxidation of lipids tend to cause a loss of function due to membrane damage to the cell and organelle membranes. In response to drought, it was observed that the

degree of cell death spiked by 3-fold compared to the degree of cell death experienced by the well-watered plants. This increase in cell death was not necessarily solely attributed to the effects of lipid peroxidation, as cysteine protease activity have a direct involvement in PCD.

Caspase-like activity detected in the leaves of the water-deprived plants suggested that the increase in cell death may have also resulted from the increase observed in the total caspase-like activity in response to drought. Since the caspase-like enzymes may be inhibited by cystatins in order to mitigate cell death, this study focused on the effects of water deficit on the gene expression of three soybean cystatins.

It was determined that drought only induced the up-regulation of a single cystatin in soybean leaves, namely, Glyma14g04250. It was also found that Glyma18g12240 was not expressed in the leaves whilst gene expression of Glyma20g08800 remained unchanged in response to drought.

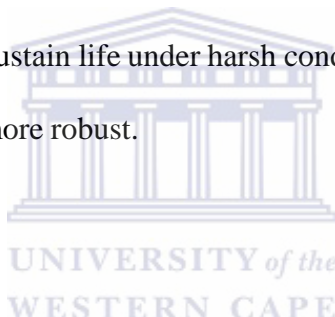
2.5. Conclusions

Various responses were exhibited by soybean plants in response to drought stress. Severe water deficit induced responses that were visible to the naked eye, such as the changes in leaf morphology and pigmentation. Molecular level changes exhibited in response to drought shed light on the important roles that cystatins play in regulating the proteolytic activities of caspase-like enzymes to modulate PCD.

In this study, it was clearly observed that water-deficit for an extended period of time led to various changes on the molecular level, which ultimately induced oxidative damage. The elevated levels of H₂O₂, degree of lipid peroxidation and the increase in caspase-like activity all contributed towards raising the level of cell death experienced by the plants exposed to conditions of drought.

The increase in cell death for a sustained period would ultimately have resulted in the death of the plants as they naturally do not possess mechanisms effective enough to alleviate the effects of oxidative stress. This was observed when only Glyma14g04250 was up-regulated in response to drought, in order to inhibit the proteolytic activity of caspase-like enzymes. However, this response was not sufficient enough to have a significant effect as the total caspase-like activity was inevitably upregulated drastically in response to water deficit.

In conclusion, cystatin proteins such as Glyma14g04250, Glyma18g12240 and Glyma20g08800 may be employed by plants to inhibit the effects of the cysteine proteases involved in the PCD pathway, but their overall effectiveness in doing so in response to drought stress is insufficient. In order for the plants to survive and sustain life under harsh conditions such as drought, the response of these cystatins may need to be more robust.



CHAPTER 3:

CHARACTERIZATION OF TWO SINGLE DOMAIN CYSTATINS, GLYMA14G04250 AND GLYMA20G08800 FROM *GLYCINE MAX*

ABSTRACT

Soybean plants are commonly produced as a crop in various parts of the world. However, irrespective of where they are grown, soybeans are susceptible to stress due to changes in the conditions of their environment. Droughts are amongst the leading causes of crop failures and heavily influence crop productivity of soybean plants. In order to improve the tolerance of soybean plants to the effects of drought, this chapter focused on characterizing the activity of two soybean cystatins, namely, Glyma14g04250 and Glyma20g08800. Following heterologous protein expression and purification of the two soybean cystatins, it was determined that both Glyma14g04250 and Glyma20g08800 displayed significant inhibitory action against the cysteine protease activity exhibited by caspase-like enzymes. It was found that the inhibition of caspase-like activity by Glyma20g08800 was more pronounced. This finding indicated that Glyma14g04250 was not as effective as Glyma20g08800 in inhibiting cysteine protease activity.

3.1. Introduction

Caspases are a group of proteins belonging to the cysteine protease family. These proteins form an integral part of the PCD pathway and apoptosis in animals, but are not present in any plant species (Estelle 2001). Plants have not evolved homologues to the caspase proteins found in animals, however, plants do possess certain cysteine proteases that perform a similar function to caspases. These proteins are referred to as caspase-like proteases which are implicated heavily in modulating programmed cell death in plants (Lam and Del Pozo 2000).

Caspase-like proteases are involved in the process of protein degradation or proteolysis (Lam and Del Pozo 2000). Therefore, enhanced levels of caspase-like activity may be detrimental to plants due to the mass degradation of proteins essential for proper cellular function. However, under favourable conditions, proteolytic degradation is essential to maintain the appropriate levels of specific proteins for optimal cellular function, as well as to control cell turnover (Kuriyama and Fukuda 2002).

Hyper activity of these proteases on the other hand is known to induce an elevated level of cell death experienced by plants, which may inevitably lead to rapid death of the organism. The expression and activity of caspase-like proteases are therefore tightly controlled by plants. Plants employ the use of various cystatins, which are proteins that inhibit cysteine proteases, in order to modulate caspase-like activity and therefore cell death (McLellan *et al.*, 2009).

The interplay between caspase-like proteases and cystatins is therefore fundamentally important to the regulation of programmed cell death in plants. This study was aimed at the characterization of two soybean cystatins, Glyma14g04250 and Glyma20g08800.

3.2. Materials and methods

3.2.1. PCR amplification and sequencing of Glyma14g04250 and Glyma20g08800

3.2.1.1. Identification and probe design of Glyma14g04250 and Glyma20g08800 using BLAST

The coding sequences for Glyma14g04250 and Glyma20g08800 full-length genes were obtained from the NCBI database (<http://www.ncbi.nlm.nih.gov/>). Primer-BLAST was then used to design primers for the PCR amplification of the Glyma14g04250 and Glyma20g08800 full-length genes. Both sets of primers were designed to contain BamHI recognition sequences on the forward primers and XhoI recognition sequences on the reverse primers to facilitate the cloning procedure. Glyma14g04250 and Glyma20g08800 were amplified using the respective primer sets according to table 1.

Table 1: Full-length primer sets for the PCR amplification and cloning of Glyma14g04250 and Glyma20g08800.

Gene	Primer Sequences
Glyma14g04250	5'- GGATCCATGGCAGCACTGGGTGGTTA -3' (Forward) 5'- CTCGAGCTAGACCGTCACCGAAAGAGGATT AACAGC -3' (Reverse)
Glyma20g08800	5'- ATGGCAGCAGTGGTGGG-3' (Forward) 5'- CTATGCAGGTGCATCTCAAACAAGCTTG -3' (Reverse)

3.2.1.2. Extraction total RNA from soybean leaves

Total RNA was extracted from soybean leaves for both well-watered and water-deprived samples using the Direct-zol™ RNA Miniprep kit (Zymo Research). Samples were prepared by homogenizing 50 mg of Soybean leaf material in a 10 times volume of TRI REAGENT®. Homogenization was performed by vortexing samples at room temperature for 1 minute to

facilitate chemical lyses of the plant cells. Cellular debris was removed from the samples via centrifugation at 10 000 x g for 2 minutes at 4° C. Supernatants obtained from centrifugation were transferred to sterile RNase-free tubes and were mixed with an equal volume of absolute ethanol (>98%) by vortexing thoroughly. The mixtures were then transferred into Zymo-spin™ IIC columns and were centrifuged for 1 minute at 10 000 x g. A prewash step was then performed on the RNA bound to the Zymo-spin™ IIC columns by the addition of Direct-zol™ RNA PreWash, followed by centrifugation for 1 minute at 10 000 x g. A second prewash step was carried out in the same manner prior to the total RNA wash step. The RNA wash was performed by the addition of RNA Wash Buffer to the Zymo-spin™IIC columns, followed by centrifugation at 10 000 x g for 1 minute. Prior to the elution of the total RNA, a centrifugation step was performed at 10 000 x g for 2 minutes in order to dry the column membranes and to facilitate the removal of excess wash buffer. The total RNA was then eluted from the Zymo-spin™ IIC columns in a final centrifugation step. Elution of the total RNA was performed by the addition of nuclease-free water, followed by centrifugation at 13 000 x g for 1 minute. Prior to the storage of the total RNA samples at -20° C, 40 U of Ribolock™ (Thermo Scientific) was added to the samples to prevent RNA degradation. RNA concentration and purity was determined by using a NanoDrop™ 1000 spectrophotometer (Thermo Scientific).

3.2.1.3. DNase treatment of total RNA samples

Total RNA samples extracted from the Soybean leaf material was subjected to a DNase treatment reaction to facilitate the degradation of contaminating DNA. DNase treatment was performed on aliquots of the total RNA samples. A total of 1 µg of RNA was subjected to DNase treatment in a reaction containing 2 U DNase I (New England Biolabs), 40 U RibolockTM (Thermo Scientific) in a 1X DNase I Reaction Buffer (New England Biolabs) made up to a final reaction volume of

30 µl with nuclease-free water. Following the setup, the reactions were incubated for 30 minutes at 37° C. Upon completion of the reaction, the DNase was heat inactivated by incubation for 5 minutes at 65° C in the presence of 0.5 mM EDTA. The RNA samples were then stored at -20° C for further use. RNA concentration and purity was determined by using a NanoDrop™ 1000 spectrophotometer (Thermo Scientific).

3.2.1.4. First strand cDNA synthesis

First strand cDNA synthesis was carried out by using the first strand cDNA synthesis kit (Thermo Scientific). The reaction setup consisted of 300 ng of template RNA, 15 pmol Oligo dT primers, 1 mM dNTPs, 20 U RibolockTM and 200 U of RevertAid in a 1x reaction buffer. Following the reaction setup, the cDNA synthesis reactions were incubated at 42° C for an hour. Upon completion of the incubation period, the reactions were terminated via heat inactivation at 80° C for 5 minutes. The samples were then stored at -20° C for further use.

3.2.1.5. Optimization of annealing temperatures for primer-specific PCR

amplification of Glyma14g04250 and Glyma20g08800

Primer sets were designed and synthesized for both the amplification of Glyma14g04250 and Glyma20g08800 full-length genes in preparation for cloning, overexpression and further downstream applications. The primer sets were designed as such that the each forward primer contained a BamHI restriction site whilst the reverse primers contained an XhoI site to facilitate the cloning procedures. Primer sets were optimized for PCR amplification by tweaking the annealing temperatures in a temperature gradient PCR setup. The PCR setup per reaction constituted of 20 µg template cDNA, 0.4 µM of forward and reverse primers, 200 nM dNTPs and 0.5 U of TrueStart Hot Start Taq polymerase in a 1X reaction buffer containing MgCl₂ (Thermo Scientific). PCR reactions were made up to a final volume of 25 µl with nuclease-free water.

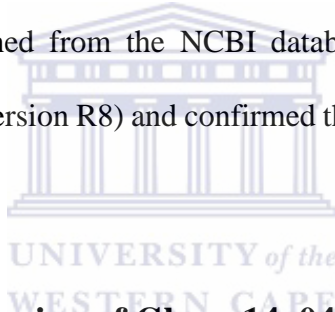
Negative controls were setup in a similar manner, with the omission of template DNA. Temperature parameters and time frames used for the PCR reactions were executed as follows. Initial denaturation was performed at 95° C for 2 minutes, then continuing onto 30 cycles of denaturation at 95° C for 30s, annealing at 56-66° C for 30s and extension at 72° C for 60s. Final extension was performed at 72° C for 7 minutes to ensure the completion of the PCR reactions. Optimal annealing temperatures for the primer sets were determined by analyzing the PCR products via gel electrophoresis for 45 minutes at 90V on a 1% agarose gel. PCR products were detected by a UV transluminator using GelRed™ (Biotium) as a visualizing agent.

3.2.1.6. High-fidelity PCR amplification of full-length soybean cystatin genes

Following the PCR optimization of the two cystatins primer sets, Glyma14g04250 and Glyma20g08800 were amplified using conventional PCR in conjunction with a high-fidelity polymerase. The Phusion® High-Fidelity PCR kit (New England Biolabs) was used for the procedure as stipulated by the manufacturer. Reaction setups constituted 40 µg cDNA in a 1x Phusion HF buffer containing 0.5 µM of the appropriate forward and reverse primers, 0.4 mM dNTPs and 1 U of Phusion Hot Start II DNA Polymerase made up to a final reaction volume of 50 µl with nuclease-free water. Negative controls were setup in the same manner, with the omission of template cDNA. Samples were then incubated in a thermocycler with the following parameters: Initial denaturation at 98° C for 30 seconds, continuing with 30 cycles of denaturation at 98° C for 10s, annealing at 64° C for 30s and extension at 72° C for 30s. A final extension step was performed at 72° C for 5 minutes to ensure completion of the PCR reactions.

3.2.1.7. Agarose gel electrophoresis, gel purification and sequencing of cystatin genes

Upon completion of the high-fidelity PCR amplification of Glyma14g04250 and Glyma20g08800, the PCR products were subjected to agarose gel electrophoresis on a 1% agarose gel at 80V for 1 hour. PCR products were then purified from the agarose gel using the GeneJet Gel Extraction kit (Thermo Scientific) as per the procedure stipulated by the manufacturer. Sequencing of the purified PCR products of Glyma14g04250 and Glyma20g08800 was outsourced to the Central Analytical Facilities sequencing service at Stellenbosch University. The sequences obtained from the sequencing procedures were then aligned to the coding sequences of Glyma14g04250 and Glyma20g08800 (previously obtained from the NCBI database) respectively. Sequences were aligned using Geneious software (Version R8) and confirmed the amplification of Glyma14g04250 and Glyma20g08800.



3.2.2. Bacterial overexpression of Glyma14g04250 and Glyma20g08800

3.2.2.1. Cloning of Glyma14g04250 and Glyma20g08800 into pET44a vector

As previously stated, the primers used for amplification of the two cystatin genes were designed to contain BamHI (G/GATCC) and XhoI (C/TCGAG) restriction sites flanking the full-length genes. In preparation of the cloning procedure, aliquots of pET44a vector as well as the purified PCR products of Glyma14g04250 and Glyma20g08800 were subjected to digestion by BamHI and XhoI restriction endonucleases. Double digest reactions were setup using 1 µg DNA in a 2X tango buffer (Thermo Scientific) containing 20 U BamHI and 10 U of XhoI made up to a reaction volume of 50 µl with nuclease-free water. The digestion reactions were then incubated at 37 °C for 4 hours, following with a termination step at 80 °C for 10 minutes. Glyma14g04250-pET44a and Glyma20g08800-pET44a plasmid constructs were then created using the Rapid DNA

Ligation kit (Thermo Scientific) as per the procedure stipulated by the manufacturer. Ligation reactions were carried out using 50 ng of the digested pET44a , with a 3:1 molar ratio (Insert:Vector) of digested Glyma14g04250 or Glyma20g08800 in a 1x Rapid Ligation buffer containing 5 U of T4 DNA ligase made up to a final volume of 20 μ l with nuclease-free water. The ligation reactions were then incubated at 25° C for 5 minutes, followed by overnight incubation at 4°C. Samples were then stored at -20° C for further use.

3.2.2.2. Transformation and growth of *E.coli* DH5 α

In order to produce additional Glyma14g04250-pET44a and Glyma0g08800-pET44a constructs for further experimentation, the newly created constructs were then transformed into Mix and Go Zymo5 α competent cells (Zymo Research). The transformation procedure was carried out as stipulated by the manufacturer. Prior to transformation, the competent cells were thawed on ice. Once the competent cells had thawed, 1 μ g of plasmid-insert construct was added to the cells, followed by gentle agitation. The transformation reactions were then spread plated onto pre-warmed LB agar plates containing Ampicillin (100 μ g/ml) before being incubated at 37° C overnight. Constructs containing Glyma14g04250 or Glyma20g08800 were confirmed by mini-preps and colony PCR before being transformed into competent cells and grown separately.

3.2.2.3. Colony PCR amplification of Glyma14g04250 and Glyma20g08800 from *E.coli* DH5 α

Following the growth of the transformants on the LB agar plates, 5 colonies were selected from each plate and were tested via colony PCRs to confirm the presence of Glyma14g04250 and Glyma20g08800. Each colony was picked and individually suspended in 5 μ l of dH₂O. 3 μ l aliquots of each of the resuspended colonies were inoculated separately into LB broth (containing 100 μ g/ml ampicillin) in order to make starter cultures. These starter cultures were incubated at 37° C for 6 hours whilst shaking at 150 rpm to facilitate growth. The remaining 2 μ l aliquots of resuspended colonies were boiled at 90° C for 5 minutes in preparation for the colony PCR. The colony PCR setup per reaction constituted of 0.4 μ M of forward and reverse primers (refer to Table 1), 200 nM dNTPs and 0.5 U of TrueStart Hot Start Taq polymerase in a 1x reaction buffer containing MgCl₂ (Thermo Scientific). PCR reactions were made up to a final volume of 25 μ l with nuclease-free water. Negative controls were setup in a similar manner, with the omission of template DNA. Temperature parameters and time frames used for the PCR reactions were executed as follows. Initial denaturation was performed at 95° C for 2 minutes, then continuing onto 30 cycles of denaturation at 95° C for 30s, annealing at 64° C for 30s and extension at 72° C for 60s. Final extension was performed at 72° C for 7 minutes to ensure the completion of the PCR reactions. Following the completion of the PCR reactions, the PCR products were analyzed via gel electrophoresis on a 1% agarose gel at 80 V for 45 minutes. GelRed® (Biotium) was used as a visualizing agent to detect the PCR products through UV transillumination.

3.2.2.4. Selective growth of transformed *E.coli* DH5 α

Starter cultures grown from colonies that were confirmed to have the desired inserts were pooled together and used to make an overnight culture for each insert. The pooled starter cultures were

inoculated into 0.1 L of LB broth containing ampicillin (100 µg/ml). A total of two overnight cultures were made from the starter cultures. One set of the cultures contained the insert Glyma14g04250 and the other contained Glyma20g08800. Following inoculation, these two cultures were incubated at 37° C overnight whilst shaking at 150 rpm to facilitate optimal growth.

3.2.2.5. Isolation of plasmid constructs from *E.coli* DH5 α

Mini-prep plasmid isolations were performed on the overnight cultures using the GeneJET Plasmid Miniprep kit (Thermo Scientific). Following the growth step, the bacterial cultures were harvested by centrifugation at 5000 x g for 10 minutes at room temperature. Liquid media was then decanted and the pelleted cells were resuspended by vortexing in Resuspension Solution. Lysis Solution was then added to the cell suspensions and was mixed by gentle agitation. Following the lysis step, Neutralization Solution was added to the mixtures and was mixed by gentle agitation once more. A centrifugation step was then performed at 12000 x g for 5 minutes in order to pellet cellular debris and the supernatants were transferred to GeneJET spin columns for a further 1 minute centrifugation. The plasmid DNA bound to the GeneJET spin columns were then washed twice by the addition of wash solution and centrifugation for 1 minute at 12000 x g. Plasmid DNA was then eluted from the GeneJET spin columns using elution buffer and centrifuging at 12000 x g for 2 minutes. Plasmid DNA concentrations and quality was determined using a NanoDrop™ 1000 spectrophotometer (Thermo Scientific). Miniprep samples were then stored at -20° C until further use.

3.2.2.6. Transformation and growth of *E.coli* BL21

Following the production and isolation of plasmid constructs from the *E.coli* DH5 α cultures, aliquots of the constructs were used to transform competent *E.coli* BL21 cells for protein overexpression of Glyma14g04250 and Glyma20g08800. One Shot® BL21 (DE3) competent cells

(Thermo Scientific) were transformed with the constructs of interest as per the procedure outlined by the manufacturer. Two samples of One Shot® BL21 (DE3) competent cells were thawed on ice. Once thawed, 500 ng of plasmid DNA (containing either Glyma14g04250 or Glyma20g08800) was added separately to the competent cells and was mixed by gentle agitation. The samples were then incubated for 30 minutes on ice before a heat shock step was administered at 42° C for 10 seconds. Following the heat shock procedure, the samples were then placed on ice once more for a period of 5 minutes. Once the 5 minutes had elapsed, the cells were inoculated into SOC media and were allowed to recover for 1 hour by incubation at 37° C with vigorous shaking (250 rpm). Following the recovery procedure, 100 µl aliquots of each sample were spread plated onto pre-warmed LB agar plates containing ampicillin (100 µg/ml) for overnight incubation at 37° C.

3.2.2.7. Colony PCR amplification of Glyma14g04250 and Glyma20g08800

from *E.coli* BL21 UNIVERSITY of the WESTERN CAPE

In preparation for protein overexpression of Glyma14g04250 and Glyma20g08800, the transformed *E.coli* BL21 colonies were screened for confirmation of the desired inserts by using colony PCR. Following the growth of the transformants on the selective LB agar plates, 5 colonies were selected from each plate and were tested via colony PCRs to confirm the presence of Glyma14g04250 and Glyma20g08800. Each colony was picked and individually suspended in 5 µl of dH₂O. 3µl aliquots of each of the resuspended colonies were inoculated separately into LB broth (containing 100 µg/ml ampicillin) in order to make starter cultures. These starter cultures were incubated at 37° C for 6 hours whilst shaking at 150 rpm to facilitate growth. The remaining

2 μ l aliquots of resuspended colonies were boiled at 90° C for 5 minutes in preparation for the colony PCR. The colony PCR setup per reaction constituted of 0.4 μ M of forward and reverse primers (refer to Table 1), 200 nM dNTPs and 0.5 U of TrueStart Hot Start Taq polymerase in a 1x reaction buffer containing MgCl₂ (Thermo Scientific). PCR reactions were made up to a final volume of 25 μ l with nuclease-free water. Negative controls were setup in a similar manner, with the omission of template DNA. Temperature parameters and time frames used for the PCR reactions were executed as follows. Initial denaturation was performed at 95° C for 2 minutes, then continuing onto 30 cycles of denaturation at 95° C for 30s, annealing at 64° C for 30s and extension at 72° C for 60s. Final extension was performed at 72° C for 7 minutes to ensure the completion of the PCR reactions. Following the completion of the PCR reactions, the PCR products were analyzed via gel electrophoresis on a 1% agarose gel at 80 V for 45 minutes. GelRed® (Biotium) was used as a visualizing agent to detect the PCR products through UV translumination.

3.2.2.8. Selective growth of transformed *E.coli* BL21 and overexpression of Glyma14g04250 and Glyma20g08800

Starter cultures grown from colonies that were confirmed to have the desired inserts were pooled together and used to make an overnight culture for each insert. The pooled starter cultures were inoculated into 0.5 L of LB broth containing ampicillin (100 μ g/ml). A total of two overnight cultures were made from the starter cultures. One set of the cultures contained the insert Glyma14g04250 and the other contained Glyma20g08800. Following inoculation, these two cultures were incubated at 37° C overnight whilst shaking at 150 rpm to facilitate optimal growth. Glycerol stocks (50%) were then made from the overnight cultures, whilst the rest was added to LB broth containing ampicillin (100 μ g/ml) and grown to an OD₆₀₀ of 0.4. Once the desired OD was reached for both cultures, overexpression of Glyma14g04250 and Glyma20g08800 was

induced by the addition of IPTG to a final concentration of 0.5 mM. Induction was facilitated by incubation of the cultures at 37° C for 16 hours, following which the cells were harvested for protein extraction. Uninduced samples were incubated at 37° C for 16 hours without the addition of IPTG.

3.2.3. Isolation and purification of Glyma14g04250 and Glyma20g08800

3.2.3.1. Isolation of total protein from *E.coli* BL21

Harvesting of the cells was performed by centrifugation at 5000 x g for 10 minutes with the pelleted cells being resuspended in 1x PBS lysis buffer. Once the cells had been completely resuspended, the samples were subjected to a freeze-thaw procedure to facilitate cell lysis for protein extraction. The freeze-thaw procedure was carried out by snap freezing the samples in liquid nitrogen, followed by thawing at 42° C. A total of 6 cycles of freeze-thawing was administered before treating the samples with DNase for 30 minutes at room temperature.

Subsequent to the DNase treatment, the samples were subjected to centrifugation at 5000 x g for 10 minutes to separate the soluble and insoluble protein fractions. The soluble and insoluble protein extracts of Glyma14g04250 and Glyma20g08800 were then stored separately at -20°C.

3.2.3.2. Affinity chromatography purification of Glyma14g04250 and Glyma20g08800 recombinant proteins

Recombinant Glyma14g04250 and Glyma20g08800 proteins were isolated from their respective soluble fractions using affinity chromatography. The recombinant proteins were purified using IMAC affinity chromatography using the Complete His-tag purification resin (Roche). An initial small-scale purification was performed for both samples to determine the optimal resin volume for purification of the Glyma14g04250 and Glyma20g08800 recombinant proteins. The purification

setups were then up-scaled to purify the entire protein extracts. For the up-scaled purifications, two columns were prepared by settling the appropriate amount of resin in the columns and allowing the excess by to be drained. Once the excess buffer had drained, the columns were equilibrated by the addition of 5 resin volumes of 1x PBS lysis buffer pH 7.4 (containing 0.14 M NaCl, 2.7 mM KCl, 8.3 mM K₂HPO₄, 1.8 mM KH₂PO₄ and 1% Triton X-100). The equilibration step was performed thrice. The total protein extracts were then added to the appropriate columns separately and were allowed to flow through the columns by gravity flow. The resin-bound proteins were then subjected to low and high stringency wash steps. The columns were washed (low stringency) thrice by the addition of 5 resin volumes of Wash buffer I (containing 50 mM Tris-HCl pH 7.5, 200 mM NaCl, 2 mM MgCl₂, 10 mM DTT and 2 mM Imidazole). A high stringency had followed by the addition of 3 resin volumes of Wash Buffer II (containing 50 mM Tris-HCl pH 7.5, 200 mM NaCl, 2 mM MgCl₂, 10 mM DTT and 7 mM Imidazole). Elution of the recombinant proteins was performed by the addition of 0.2 resin volumes of Elution buffer (containing 50 mM Tris-HCl pH 7.5, 200 mM NaCl, 2 mM MgCl₂, 10 mM DTT and 400 mM Imidazole). to both columns. The eluted proteins were collected in 1 ml fractions before storage at -20°C.

3.2.3.3. Cleavage of recombinant proteins and purification of Glyma14g04250 and Glyma20g08800

In preparation for cleavage, the purified recombinant proteins were exchanged into a 50 mM Tris (pH 8.0) buffer containing 10 mM CaCl₂. Cleavage of the recombinant proteins was performed using the Thrombin CleanCleave™ kit (Sigma-Aldrich) as per the procedure outlined by the manufacturer. Suspensions (50%) of thrombin-agarose were prepared by pelleting the resin through centrifugation at 500 x g for 2 minutes. The resin was then washed by the addition of 1x Cleavage buffer and gentle agitation before removal of the buffer by pipetting after centrifugation

at 500 x g for 2 minutes. In order to facilitate the cleavage reactions, the washed resin were resuspended in 10X cleavage buffer by gentle agitation. 1 mg of recombinant protein was added to the resin and was made up to a final volume of 1 ml using nuclease-free water. The cleavage reactions were incubated for 16 hours at room temperature with gentle agitation. Once the incubation period had expired, the cleaved proteins were recovered by centrifugation at 500 x g for 5 minutes. Prior to storage -20° C, the proteins of interest were purified once more using affinity chromatography column setups as per the abovementioned procedure. During the final purification, the proteins of interest were collected as the flow-through from the columns instead of by elution. The remaining peptides cleaved from the proteins of interest contained the His tags and therefore remained bound to the resin whilst only allowing Glyma14g04250 and Glyma20g08800 to bypass the resin to be collected.

3.2.3.4. Analysis of purified proteins via SDS-PAGE gel electrophoresis

Prior to the testing of Glyma14g04250 and Glyma20g08800 activity, the total protein extracts of the uninduced and induced samples were analyzed alongside the purified proteins using SDS-PAGE gel electrophoresis (Figure 18). Aliquots of the protein samples were electrophoresed at 120 V for 2 hours on 12% polyacrylamide gels. Following gel electrophoresis, proteins were visualized by staining using Coomassie Brilliant Blue R-250 Dye (Thermo Scientific). The staining procedure was executed by incubating the gels for 15 minutes in boiled Coomassie solution with shaking. After the staining step, the gels were allowed to destain in a 20% acetic acid solution overnight.

3.2.3.5. Characterization of Glyma14g04250 and Glyma20g08800 activity

Glyma14g04250 and Glyma20g08800 activities were determined by measuring changes in the total caspase-like activity of a protein extract when being supplemented with either of the two

cystatins. A protein extraction procedure was performed by homogenizing a total of 100mg of leaf tissue (well-watered leaf material) in a 5 times volume (w/v) of protein extraction buffer (containing 5% glycerol, 10% PVPP and 100 mM Tris pH 8.0). Total proteins were isolated from the cellular debris by centrifugation at 10000 x g for 15 minutes at 4° C. The total protein extract was then used to assay the inhibitory activity of Glyma14g04250 and Glyma20g08800. Caspase-like activity was detected through the selective inhibition of the threonine and serine proteases within the protein extracts being tested. This was achieved by the addition of 1 mM PMSF to 50µg samples of total protein whilst the addition of 10 mM β-mercaptoethanol reversed the inhibition of cysteine proteases by PMSF. Reaction setups consisted of one sample for the total caspase-like activity of the extract, whilst the second and third samples were supplemented with 10 µg of purified Glyma14g04250 and Glyma20g08800 respectively. The samples were then incubated for 5 minutes at 37° C. Following the incubation period, 0.5 mM Ac-DEVD-pNA (Sigma Aldrich) was then added to the samples before incubation for 60 minutes at 37° C. Total caspase-like activity was measured spectrophotometrically at 405 nm via the detection of p-nitroaniline (extinction coefficient 9.6mM⁻¹.cm⁻¹). Absorbance readings were measured in 10 minute intervals for the duration of the incubation.

3.3. Results

3.3.1. Screening of transformed *E.coli* DH5α AND BL21 for target genes

Colony PCR was used to screen transformed *E.coli* DH5α and BL21 colonies for the target inserts Glyma14g04250 and Glyma20g08800 (Tables 2 and 3). A total of 5 *E.coli* DH5α and BL21 colonies each were picked and screened for the two cystatin target genes. Screening of the *E.coli* DH5α and BL21 colonies detected the presence of the target genes in each of the colonies whilst the negative controls detected no amplification. Since all of the negative controls resulted in no

amplification, it was concluded that only the desired target genes (Glyma14g04250 and Glyma20g08800) had been amplified from both *E.coli* DH5 α and BL21 colonies.

Table 2: Screening of *E.coli* DH5 α transformants for Glyma14g04250 and Glyma20g08800 using Colony PCR

Colonies	Glyma14g04250	Glyma20g08800	Negative Controls
Colony 1	+	+	-
Colony 2	+	+	-
Colony 3	+	+	-
Colony 4	+	+	-
Colony 5	+	+	-

Key:
Amplification (+)
No amplification (-)

Table 3: Screening of *E.coli* BL21 transformants for Glyma14g04250 and Glyma20g08800 using Colony PCR

Colonies	Glyma14g04250	Glyma20g08800	Negative Controls
Colony 1	+	+	-
Colony 2	+	+	-
Colony 3	+	+	-
Colony 4	+	+	-
Colony 5	+	+	-

Key:
Amplification (+)
No amplification (-)

3.3.2. SDS-PAGE analysis of protein purification by affinity chromatography

Following the successful overexpression of Glyma14g04250 and Glyma20g08800 in *E.coli* BL21, the proteins of interest were purified by affinity chromatography and analyzed by SDS-PAGE gel electrophoresis (figure 18). The recombinant proteins containing either Glyma14g04250 or Glyma20g08800 had an estimated size of approximately 80 kDa. Crude total protein extracts from uninduced and induced *E.coli* BL21 were electrophoresed alongside one another on a 12% SDS-Polyacrylamide gel. The expression of the target proteins in the uninduced crude extracts were at levels similar to that of the proteins native to the bacteria. However, crude extracts from the induced samples showed highly overexpressed proteins that were approximately 80 kDa in size, implicating the proteins of interest. The crude extracts containing the overexpressed recombinant proteins were purified and were subjected to cleavage to release Glyma14g04250 and Glyma20g08800. Pure extracts of Glyma14g04250 and Glyma20g08800 were analyzed via SDS-PAGE (figure 18). As displayed in figure 18, the purified proteins of interest both corresponded to the expected molecular weight of ~11.4 kDa, confirming that the proteins of interest were purified successfully.

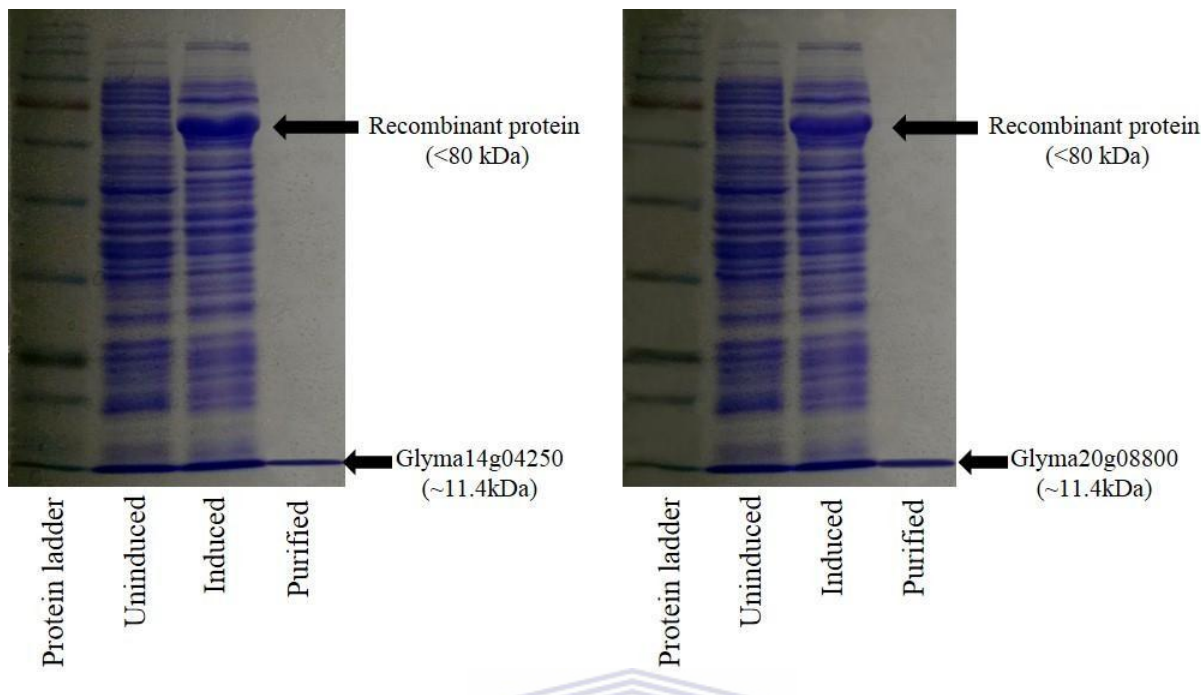


Figure 18: SDS-PAGE analysis of protein purification by affinity chromatography. Crude total protein extracts and purified target proteins were subjected to SDS-PAGE gel electrophoresis. Lane 1 contained a protein ladder while lanes 2-4 contained the uninduced crude extracts, induced crude extracts and the cleaved and purified target proteins respectively.

3.3.3. Detection of Glyma14g04250 and Glyma20g08800 inhibitory action on total caspase-like activity from soybean leaves

The activities of Glyma14g04250 and Glyma20g08800 were tested against total caspase-like activity in a total protein extract from well-watered leaves (Figure 19). A caspase-like activity assay was used to ascertain whether Glyma14g04250 and Glyma20g08800 showed inhibitory action against cysteine proteases. The results generated showed that Glyma14g04250 and Glyma20g08800 inhibited total caspase-like activity quite significantly (figure 19). Glyma20g08800 showed a more potent inhibitory action against the cysteine protease activity of the caspase-like enzymes within the total protein extract. Without the presence of either

Glyma14g04250 or Glyma20g08800, the total caspase-like activity observed was $\pm 15 \mu\text{mol}.\text{min}.\text{mg}^{-1}$ FW. However, in the presence of 10 μg of Glyma14g04250 and Glyma20g08800, total caspase-like activity is diminished to $\pm 10 \mu\text{mol}.\text{min}.\text{mg}^{-1}$ FW (33% decline in activity) and $\pm 8 \mu\text{mol}.\text{min}.\text{mg}^{-1}$ FW (47% decline in activity) as displayed in figure 19.

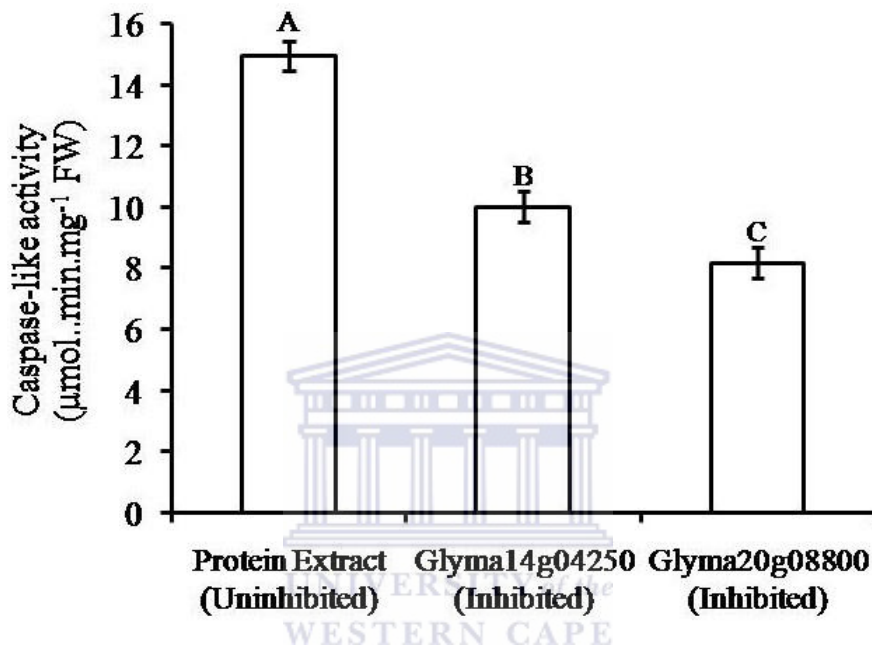


Figure 19: Quantification of the inhibitory activities of Soybean cystatins Glyma14g04250 and Glyma20g08800. Total caspase-like activity of a protein extract from well-watered Soybean leaves was measured in the absence and presence of inhibitors. The uninhibited sample was representative of the total caspase-like activity, whilst the inhibited samples contained 10 μg of Glyma14g04250 and Glyma20g08800 respectively. Error bars were generated using the means \pm SE for three independent experiments.

3.4. Discussion

The experimental work performed during this chapter of the research project was aimed at ultimately overexpressing two soybean cystatins and confirming their inhibitory action against cysteine proteases such as caspase-like enzymes. The cloning and transformation procedures were relatively straightforward and highly efficient as observed during the screening procedures.

Out of the colony selection during the screening procedure, it was observed that the entirety of the selection contained the genes of interest (Tables 2 and 3) which was indicative of a high efficiency in the procedure. During the overexpression of the two cystatins, it was observed by SDS-PAGE analysis that the majority of the overexpressed proteins were found in the soluble protein fractions.

With that being said, it was also observed that a significant amount of the recombinant proteins were present in the insoluble protein fractions as well. This suggested the possibility that the recombinant proteins were overexpressed at such high levels that they were forced into inclusion bodies. The proteins of interest contained within the soluble fraction were subjected to purification by affinity chromatography and cleavage by thrombin.

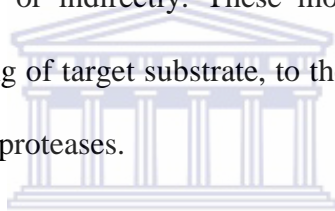
Following the successful purification and cleavage of the recombinant proteins, the proteins of interest (Glyma14g04250 and Glyma20g08800) were successfully isolated via a second purification step. Total protein crude extracts of uninduced and induced samples were analyzed by SDS-PAGE gel electrophoresis alongside purified Glyma14g04250 and Glyma20g08800.

The purified proteins were confirmed to be the proteins of interest as their actual size of 11.4kDa matched that of their expected sizes. Successful isolation of the purified cystatins was an important step in preparation for the testing of their activity against cysteine protease activity. Considering that caspase-like enzymes are well known to be cysteine proteases, inhibitory activities of

Glyma14g04250 and Glyma20g08800 were tested against caspase-like enzymes isolated from soybean leaves.

Through experimentation, it was revealed that the cystatins had in fact displayed inhibition of the proteolytic activity exhibited by caspase-like enzymes. Even though both cystatins inhibited caspase-like activity, it was observed that Glyma20g08800 was more effective than Glyma14g04250 in doing so. This difference in effectiveness may have been attributed to the mode of action of Glyma14g04250 and Glyma20g08800 during the process of inhibition.

According to Rzychon *et al.*, (2004), cystatins display various modes of action that may inhibit cysteine protease activity directly or indirectly. These modes of action range from indirect inhibition such as backward binding of target substrate, to the involvement of inhibition through direct interaction with the cysteine proteases.



Direct modes of action for cystatins may involve the distortion of the target protein active sites, allosteric inhibition or covalent bonding to the cysteine proteases. Cystatins may act by blocking or distorting the active sites, restricting the access of substrates to the cysteine protease catalytic centres. Ultimately, cystatin modulated inhibition of cysteine protease activity is attributed to a change in conformation of the substrates or cysteine proteases themselves.

3.5. Conclusions

The results generated by this study showed substantial evidence of the inhibitory actions of Glyma14g04250 and Glyma20g08800 against cysteine protease activities of caspase-like enzymes. The heterologous protein expression system used for the overexpression of the two cystatins showed no negative effects, such as incorrect protein folding, on the activity of the cystatins.

Although Glyma20g08800 displayed a higher effectiveness than Glyma14g04250 at inhibiting the proteolytic activities of caspase-like enzymes, the exact reason behind this may need to be further investigated. Only by assumption could we speculate that the difference observed in cystatin activity may have been due to differences in modes of action for Glyma14g04250 and Glyma20g08800. Alternatively, it was plausible that this feat may have been a result of the two cystatins possessing different affinities for their respective targets.

Bibliography

1. Alscher, R. G., Erturk, N., & Heath, L. S. (2002). Roles of superoxide dismutases (SODs) in controlling oxidative stress in plants. *J. Exp. Bot.* 53, 1331-1341.
2. Anjum, S. A., Xie, X. Y., Wang, L. C., Saleem, M. F., Man, C., & Lei, W. (2011). Morphological, physiological and biochemical responses of plants to drought stress. *African Journal of Agricultural Research*, 6(9), 2026-2032.
3. Apel, K. and H. Hirt (2004). "Reactive oxygen species: metabolism, oxidative stress, and signal transduction." *Annu. Rev. Plant Biol.* 55: 373-399.
4. Asada, K. (2006). "Production and scavenging of reactive oxygen species in chloroplasts and their functions." *Plant Physiology*, 141(2): 391-396.
5. Ashraf, M., & Iram, A. (2005). Drought stress induced changes in some organic substances in nodules and other plant parts of two potential legumes differing in salt tolerance. *Flora-Morphology, Distribution, Functional Ecology of Plants*, 200(6), 535-546.
6. Baek, K. H., & Choi, D. (2008). Roles of plant proteases in pathogen defense. *Plant Pathology Journal*, 24, 367-374.
7. Barker‡, M. and M. Carr (1989). "Teaching and learning about photosynthesis. Part 1: An assessment in terms of students' prior knowledge." *International Journal of Science Education* 11(1): 49-56.
8. Beers, E. P., & McDowell, J. M. (2001). Regulation and execution of programmed cell death in response to pathogens, stress and developmental cues. *Current opinion in plant biology*, 4(6), 561-567.
9. Britt, A. B. (1999). Molecular genetics of DNA repair in higher plants. *Trends in plant science*, 4(1), 20-25.
10. Buxbaum, E. (2007). *Fundamentals of protein structure and function*. Springer.
11. Challinor, A. J., Simelton, E. S., Fraser, E. D., Hemming, D., & Collins, M. (2010). Increased crop failure due to climate change: assessing adaptation options using models and socio-economic data for wheat in China. *Environmental Research Letters*, 5(3), 034012.

12. Chaves, M. M., Maroco, J. P., & Pereira, J. S. (2003). Understanding plant responses to drought—from genes to the whole plant. *Functional plant biology*, 30(3), 239-264.
13. Chen, Q., Vazquez, E. J., Moghaddas, S., Hoppel, C. L., & Lesnefsky, E. J. (2003). Production of reactive oxygen species by mitochondria central role of complex III. *Journal of Biological Chemistry*, 278(38), 36027-36031.
14. Choudhury, S., Panda, P., Sahoo, L., & Panda, S. K. (2013). Reactive oxygen species signaling in plants under abiotic stress. *Plant signaling&behavior*, 8(4), e23681.
15. Collazo, C., Chacón, O., & Borrás, O. (2006). Programmed cell death in plants resembles apoptosis of animals. *Biología Aplicada*, 23, 1-10.
16. Corpas, F. J., Barroso, J. B., & del Río, L. A. (2001). Peroxisomes as a source of reactive oxygen species and nitric oxide signal molecules in plant cells. *Trends in plant science*, 6(4), 145-150.
17. Croft, K. P. C., Voisey, C. R., & Slusarenko, A. J. (1990). Mechanism of hypersensitive cell collapse: correlation of increased lipoxygenase activity with membrane damage in leaves of Phaseolus vulgaris (L) inoculated with an avirulent race of Pseudomonas syringae pv. phaseolicola. *Physiological and Molecular Plant Pathology*, 36(1), 49-62.
18. Dangl, J. L., & Jones, J. D. (2001). Plant pathogens and integrated defence responses to infection. *nature*, 411(6839), 826-833.
19. Danon, A., Rotari, V. I., Gordon, A., Mailhac, N., & Gallois, P. (2004). Ultraviolet-C overexposure induces programmed cell death in Arabidopsis, which is mediated by caspase-like activities and which can be suppressed by caspase inhibitors, p35 and Defender against Apoptotic Death. *Journal of Biological Chemistry*, 279(1), 779-787.
20. D'Autréaux, B., & Toledano, M. B. (2007). ROS as signalling molecules: mechanisms that generate specificity in ROS homeostasis. *Nature Reviews Molecular Cell Biology*, 8(10), 813-824.
21. De Gara, L., Locato, V., Dipierro, S., & de Pinto, M. C. (2010). Redox homeostasis in plants. The challenge of living with endogenous oxygen production. *Respiratory physiology & neurobiology*, 173, S13-S19.
22. De Jong, A. J., Hoeberichts, F. A., Yakimova, E. T., Maximova, E., & Woltering, E. J. (2000). Chemical-induced apoptotic cell death in tomato cells: involvement of caspase-like proteases. *Planta*, 211(5), 656-662.
23. del Río, L. A., Sandalio, L. M., Corpas, F. J., Palma, J. M., & Barroso, J. B. (2006). Reactive oxygen species and reactive nitrogen species in peroxisomes. Production, scavenging, and role in cell signaling. *Plant Physiology*, 141(2), 330-335.
24. del Rio, L.A., Sandalio, L.M., Altomare, D.A., & Zilinskas, B.A. (2003) Mitochondrial and peroxisomal magnese superoxide dismutase: differential expression during leaf senescence, *J. Exp. Bot.* 54, 923-933.
25. Estelle, M. (2001). Proteases and cellular regulation in plants. *Current opinion in plant biology*, 4(3), 254-260.
26. Fattah, F., Lee, E. H., Weisensel, N., Wang, Y., Lichter, N., & Hendrickson, E. A. (2010). Ku regulates the non-homologous end joining pathway choice of DNA double-strand break repair in human somatic cells. *PLoS genetics*, 6(2), e1000855.
27. Ferreira, R. R., Fornazier, R. F., Vitoria, A. P., Lea, P. J., & Azevedo, R. A. (2002). Changes in antioxidant enzyme activities in soybean under cadmium stress. *J. Plant Nutr.* 25, 327-342.
28. Finkel, T. (2000). Redox-dependent signal transduction. *FEBS letters*, 476(1), 52-54.

29. Finkel, T. (2011). Signal transduction by reactive oxygen species. *The Journal of cell biology*, 194(1), 7-15.
30. Finkel, T., & Holbrook, N. J. (2000). Oxidants, oxidative stress and the biology of ageing. *Nature*, 408(6809), 239-247.
31. Foyer, C. H., & Noctor, G. (2003). Redox sensing and signalling associated with reactive oxygen in chloroplasts, peroxisomes and mitochondria. *Physiologia Plantarum*, 119(3), 355-364.
32. Fukuyama, H., & Le Bihan, D. (2010). *Water: the forgotten biological molecule*. Pan Stanford Publishing.
33. García-Carreño, F. L. (1992). Protease inhibition in theory and practice. *Biotechnology Education*, 3(4), 145-150.
34. Ghezzi, P., & Bonetto, V. (2003). Redox proteomics: identification of oxidatively modified proteins. *Proteomics*, 3(7), 1145-1153.
35. Gill, S. S. and N. Tuteja (2010). "Reactive oxygen species and antioxidant machinery in abiotic stress tolerance in crop plants." *Plant Physiology and Biochemistry* 48(12): 909-930.
36. Gill, S. S., & Tuteja, N. (2011). Cadmium stress tolerance in crop plants: probing the role of sulfur. *Plant signaling&behavior*, 6(2), 215-222.
37. Grimsrud, P. A., Xie, H., Griffin, T. J., & Bernlohr, D. A. (2008). Oxidative stress and covalent modification of protein with bioactive aldehydes. *Journal of Biological Chemistry*, 283(32), 21837-21841.
38. Gruber, S., Emrich, K., & Claupein, W. (2009). Classification of canola (*Brassica napus*) winter cultivars by secondary dormancy. *Canadian Journal of Plant Science*, 89(4), 613-619.
39. Gutteridge, J. M. (1995). Lipid peroxidation and antioxidants as biomarkers of tissue damage. *Clinical chemistry*, 41(12), 1819-1828.
40. Habib, H., & Fazili, K. M. (2007). Plant protease inhibitors: a defense strategy in plants. *Biotechnology and Molecular Biology Review*, 2(3), 68-85.
41. Harvey, B. and R. Downey (1964). "The inheritance of erucic acid content in rapeseed (*Brassica napus*)." *Canadian Journal of Plant Science* 44(1): 104-111.
42. Hatsugai, N., Kuroyanagi, M., Yamada, K., Meshi, T., Tsuda, S., Kondo, M., ...& Hara-Nishimura, I. (2004). A plant vacuolar protease, VPE, mediates virus-induced hypersensitive cell death. *Science*, 305(5685), 855-858.
43. Hemnani, T., & Parihar, M. S. (1998). Reactive oxygen species and oxidative DNA damage. *Indian journal of physiology and pharmacology*, 42(4), 440-452.
44. Holmberg, N., & Bülow, L. (1998). Improving stress tolerance in plants by gene transfer. *Trends in plant science*, 3(2), 61-66.
45. Hossain, M. A., da Silva, J. A. T., & Fujita, M. (2011). Glyoxalase system and reactive oxygen species detoxification system in plant abiotic stress response and tolerance: an intimate relationship.
46. Huang, A. H. (Ed.). (1983). *Plant peroxisomes*. Access Online via Elsevier.
47. Irigoyen, J. J., Emerich, D. W., & Sánchez-Díaz, M. (1992). Alfalfa leaf senescence induced by drought stress: photosynthesis, hydrogen peroxide metabolism, lipid peroxidation and ethylene evolution. *Physiologia Plantarum*, 84(1), 67-72.
48. Jacobson, M. D., Weil, M., & Raff, M. C. (1997). Programmed cell death in animal development. *Cell*, 88(3), 347-354.

49. Jones, P. J., & Papamandjaris, A. A. (2012). Lipids: cellular metabolism. *Present Knowledge in Nutrition, Tenth Edition*, 132-148.
50. Keyvan, S. (2010). The effects of drought stress on yield, relative water content, proline, soluble carbohydrates and chlorophyll of bread wheat cultivars. *J. Anim. Plant Sci*, 8(3), 1051-1060.
51. Kuriyama, H., & Fukuda, H. (2002). Developmental programmed cell death in plants. *Current opinion in plant biology*, 5(6), 568-573.
52. Lam, E., & Del Pozo, O. (2000). Caspase-like protease involvement in the control of plant cell death. In *Programmed Cell Death in Higher Plants* (pp. 173-184). Springer Netherlands.
53. Lea, C., Lowrie, P., & McGuigan, S. (2000). *AS Biology: For AQA Specification B*. Heinemann.
54. Letey, J. (1985). Relationship between soil physical properties and crop production. Advances in soil science, Springer: 277-294.
55. Limón-Pacheco, J., & Gonsebatt, M. E. (2009). The role of antioxidants and antioxidant-related enzymes in protective responses to environmentally induced oxidative stress. *Mutation Research/Genetic Toxicology and Environmental Mutagenesis*, 674(1), 137-147.
56. Lodish, H., Berk, A., Zipursky, S. L., Matsudaira, P., Baltimore, D., & Darnell, J. (2000). Cell death and its regulation.
57. Loeb, L. A., Wallace, D. C., & Martin, G. M. (2005). The mitochondrial theory of aging and its relationship to reactive oxygen species damage and somatic mtDNA mutations. *Proceedings of the National Academy of Sciences of the United States of America*, 102(52), 18769-18770.
58. Luis, A., Corpas, F. J., Sandalio, L. M., Palma, J. M., Gómez, M., & Barroso, J. B. (2002). Reactive oxygen species, antioxidant systems and nitric oxide in peroxisomes. *Journal of Experimental Botany*, 53(372), 1255-1272.
59. Mao, G. D., & Poznansky, M. J. (1992). Electron spin resonance study on the permeability of superoxide radicals in lipid bilayers and biological membranes. *FEBS letters*, 305(3), 233-236.
60. Mao, G. D., Thomas, P. D., Lopaschuk, G. D., & Poznansky, M. J. (1993). Superoxide dismutase (SOD)-catalase conjugates. Role of hydrogen peroxide and the Fenton reaction in SOD toxicity. *Journal of Biological Chemistry*, 268(1), 416-420.
61. Martinez, M., Diaz-Mendoza, M., Carrillo, L., & Diaz, I. (2007). Carboxy terminal extended phytocystatins are bifunctional inhibitors of papain and legumain cysteine proteinases. *FEBS letters*, 581(16), 2914-2918.
62. McLellan, H., Gilroy, E. M., Yun, B. W., Birch, P. R., & Loake, G. J. (2009). Functional redundancy in the Arabidopsis Cathepsin B gene family contributes to basal defence, the hypersensitive response and senescence. *New Phytologist*, 183(2), 408-418.
63. Miransari, M. (2010). "Contribution of arbuscularmycorrhizal symbiosis to plant growth under different types of soil stress." *Plant Biology* 12(4): 563-569.
64. Mittler, R. (2002). Oxidative stress, antioxidants and stress tolerance. *Trends in plant science*, 7(9), 405-410.
65. Mittler, R., Vanderauwera, S., Gollery, M., & Van Breusegem, F. (2004). Reactive oxygen gene network of plants. *Trends in plant science*, 9(10), 490-498.
66. Miwa, S., & Brand, M. D. (2003). Mitochondrial matrix reactive oxygen species production is very sensitive to mild uncoupling. *Biochemical Society Transactions*, 31(6), 1300-1301.

67. Møller, I. M. (2001). Plant mitochondria and oxidative stress: electron transport, NADPH turnover, and metabolism of reactive oxygen species. *Annual review of plant biology*, 52(1), 561-591.
68. Møller, I. M., Jensen, P. E., & Hansson, A. (2007). Oxidative modifications to cellular components in plants. *Annu. Rev. Plant Biol.*, 58, 459-481.
69. Mullineaux, P. M., & Baker, N. R. (2010). Oxidative stress: antagonistic signaling for acclimation or cell death?. *Plant physiology*, 154(2), 521-525.
70. Nielsen, S. L., & Simonsen, A. M. (2011). Photosynthesis and photoinhibition in two differently coloured varieties of *Oxalis triangularis*—the effect of anthocyanin content. *Photosynthetica*, 49(3), 346-352.
71. Noctor, G., & Foyer, C. H. (1998). A re-evaluation of the ATP: NADPH budget during C3 photosynthesis. A contribution from nitrate assimilation and its associated respiratory activity? *J. Exp. Bot.* 49, 1895-1908.
72. Oda, K. (2012). New families of carboxyl peptidases: serine-carboxyl peptidases
73. Ohsawa, I., Ishikawa, M., Takahashi, K., Watanabe, M., Nishimaki, K., Yamagata, K., ...&Ohta, S. (2007). Hydrogen acts as a therapeutic antioxidant by selectively reducing cytotoxic oxygen radicals. *Nature medicine*, 13(6), 688-694.
74. Oliveira, A. S., Xavier-Filho, J., & Sales, M. P. (2003). Cysteine proteinases and cystatins. *Brazilian Archives of Biology and Technology*, 46(1), 91-104.
75. Oomah, B. D. and G. Mazza (1999). "Health benefits of phytochemicals from selected Canadian crops." *Trends in Food Science & Technology* 10(6): 193-198.
76. Pernas, M., Sánchez-Monge, R., & Salcedo, G. (2000). Biotic and abiotic stress can induce cystatin expression in chestnut. *FEBS letters*, 467(2), 206-210.
77. Proskuryakov, S. Y., Konoplyannikov, A. G., & Gabai, V. L. (2003). Necrosis: a specific form of programmed cell death?. *Experimental cell research*, 283(1), 1-16.
78. Puntarulo, S., Sánchez, R. A., & Boveris, A. (1988). Hydrogen peroxide metabolism in soybean embryonic axes at the onset of germination. *Plant Physiology*, 86(2), 626-630.
79. Rai, A. K., & Takabe, T. (2006). *Abiotic stress tolerance in plants* (pp. 121-133). Springer.
80. Ray, P. D., Huang, B. W., & Tsuji, Y. (2012). Reactive oxygen species (ROS) homeostasis and redox regulation in cellular signaling. *Cellular signalling*, 24(5), 981-990.
81. Rissler, J. And M. Margaret (1996). "The ecological risks of engineered crops", MIT Press. pp 93-102.
82. Ruest, L. B., Khalyfa, A., & Wang, E. (2002). Development-dependent disappearance of caspase-3 in skeletal muscle is post-transcriptionally regulated. *Journal of cellular biochemistry*, 86(1), 21-28.
83. Rzychon, M., Chmiel, D., & Stec-Niemczyk, J. (2004). Modes of inhibition of cysteine proteases. *Acta Biochim. Pol*, 51(4), 861-873.
84. Sharma, I. (2012). Arsenic induced oxidative stress in plants. *Biologia*, 67(3), 447-453.
85. Sharma, P., Jha, A. B., Dubey, R. S., & Pessarakli, M. (2012). Reactive oxygen species, oxidative damage, and antioxidative defense mechanism in plants under stressful conditions. *Journal of botany*, 2012.
86. Soares-Costa, A., Beltramini, L. M., Thiemann, O. H., & Henrique-Silva, F. (2002). A sugarcane cystatin: recombinant expression, purification, and antifungal activity. *Biochemical and biophysical research communications*, 296(5), 1194-1199.

87. Solomon, M., Belenghi, B., Delledonne, M., Menachem, E., & Levine, A. (1999). The involvement of cysteine proteases and protease inhibitor genes in the regulation of programmed cell death in plants. *The Plant Cell*, 11(3), 431-443.
88. Steyn, W. J., Wand, S. J. E., Holcroft, D. M., & Jacobs, G. (2002). Anthocyanins in vegetative tissues: a proposed unified function in photoprotection. *New Phytologist*, 155(3), 349-361.
89. Suzuki, N., Koussevitzky, S. H. A. I., Mittler, R. O. N., & Miller, G. A. D. (2012). ROS and redox signalling in the response of plants to abiotic stress. *Plant, Cell & Environment*, 35(2), 259-270.
90. Tate, E. and A. Gustard (2000). Drought definition: a hydrological perspective, Springer.
91. Tuteja, N. (2007). "Mechanisms of high salinity tolerance in plants." Methods in enzymology **428**: 419.
92. Tuteja, N., Singh, M. B., Misra, M. K., Bhalla, P. L., & Tuteja, R. (2001). Molecular mechanisms of DNA damage and repair: progress in plants. *Critical Reviews in Biochemistry and Molecular Biology*, 36(4), 337-397.
93. Valko, M., Rhodes, C. J., Moncol, J., Izakovic, M. M., & Mazur, M. (2006). Free radicals, metals and antioxidants in oxidative stress-induced cancer. *Chemico-biological interactions*, 160(1), 1-40.
94. Vidaver, A. K., & Lambrecht, P. A. (2004). Bacteria as plant pathogens. *The plant health Instructor*.
95. Wiseman, H., & Halliwell, B. (1996). Damage to DNA by reactive oxygen and nitrogen species: role in inflammatory disease and progression to cancer. *Biochem. J*, 313, 17-29.
96. Zepplin, R. G., Faust, B. C., & Hoigne, J. (1992). Hydroxyl radical formation in aqueous reactions (pH 3-8) of iron (II) with hydrogen peroxide: the photo-Fenton reaction. *Environmental Science & Technology*, 26(2), 313-319.